AD NUMBER

ADB013236

LIMITATION CHANGES

TO:

Approved for public release; distribution is unlimited.

FROM:

Distribution authorized to U.S. Gov't. agencies only; Test and Evaluation; OCT 1975. Other requests shall be referred to Air Force Flight Dynamics Laboratory, Wright-Patterson AFB, OH 45433.

AUTHORITY

AFFDL ltr, 27 Dec 1977

AFFDL-TR-76-49
Volume I

AD B013236

FINITE ELEMENT ANALYSIS OF TRANSONIC FLOWS OVER THIN AIRFOILS VOLUME I - FINAL REPORT

LOCKHEED MISSILES & SPACE COMPANY, INC.
HUNTSVILLE RESEARCH & ENGINEERING CENTER
4800 BRADFORD DRIVE, HUNTSVILLE, AL 35807

MAY 1976

FINAL REPORT FOR PERIOD JULY 1975 – MARCH 1976

AIR FORCE FLIGHT DYNAMICS LABORATORY
AIR FORCE WRIGHT AERONAUTICAL LABORATORIES
AIR FORCE SYSTEMS COMMAND
WRIGHT-PATTERSON AIR FORCE BASE, OHIO 45433

NOTICE

When Government drawings, specifications, or other data are used for any purpose other than in connection with a definitely related Government procurement operation, the United States Government thereby incurs no responsibility nor any obligation whatsoever; and the fact that the government may have formulated, furnished, or in any way supplied the said drawings, specifications, or other data, is not to be regarded by implication or otherwise in any manner licensing the holder or any other person or corporation, or conveying any rights or permission to manufacture, use, or sell any patented invention that may in any way be related thereto.

This technical report has been reviewed and is approved for publication.

Gerald M Van Keuren

GERALD M. VAN KEUREN, CAPT, USAF
Project Engineer

FOR THE COMMANDER

Gerald G. Leigh

GERALD G. LEIGH, Lt. Col., USAF
Chief, Structures Division

Copies of this report should not be returned unless return is required by security considerations, contractual obligations, or notice on a specific document.

AIR FORCE - 20 AUGUST 76 - 100

UNCLASSIFIED

SECURITY CLASSIFICATION OF THIS PAGE (When Data Entered)

REPORT DOCUMENTATION PAGE

READ INSTRUCTIONS BEFORE COMPLETING FORM

1. REPORT NUMBER: AFFDL-TR-76-49-Volume I-1	2. GOVT ACCESSION NO.
3. RECIPIENT'S CATALOG NUMBER	
4. TITLE (and Subtitle): FINITE ELEMENT ANALYSIS OF TRANSONIC FLOWS OVER THIN AIRFOILS. VOLUME I, FINAL REPORT	5. TYPE OF REPORT & PERIOD COVERED: Final Report. July 1975 – March 1976
	6. PERFORMING ORG. REPORT NUMBER: LMSC-HREC TR D496713-1
7. AUTHOR(s): S. T. K. Chan, H. C. Chen, and M. R. Brashears	8. CONTRACT OR GRANT NUMBER(s): F33615-75-C-3125
9. PERFORMING ORGANIZATION NAME AND ADDRESS: Lockheed Missiles & Space Company, Inc. Huntsville Research & Engineering Center Huntsville, Ala. 35807	10. PROGRAM ELEMENT, PROJECT, TASK AREA & WORK UNIT NUMBERS: Project 1370 Task 13700414
11. CONTROLLING OFFICE NAME AND ADDRESS: Air Force Flight Dynamics Laboratory Vehicle Dynamics Division Wright-Patterson AFB, Ohio 45433	12. REPORT DATE: May 1976
	13. NUMBER OF PAGES: 68
14. MONITORING AGENCY NAME & ADDRESS (if different from Controlling Office): Same as above. 69 p.	15. SECURITY CLASS. (of this report): Unclassified
	15a. DECLASSIFICATION/DOWNGRADING SCHEDULE

16. DISTRIBUTION STATEMENT (of this Report)

Distribution limited to U.S. Government agencies only; test and evaluation statement applied October 1975. Other requests for this document must be referred to AF Flight Dynamics Laboratory (FBR), Wright-Patterson Air Force Base, Ohio 45433.

17. DISTRIBUTION STATEMENT (of the abstract entered in Block 20, if different from Report)

N/A AF-1370 1370404

18. SUPPLEMENTARY NOTES

N/A

19. KEY WORDS (Continue on reverse side if necessary and identify by block number)

Steady Transonic Flow — Potential Flow — Method of Weighted Residuals

Unsteady Transonic Flow — Finite Element Method

20. ABSTRACT (Continue on reverse side if necessary and identify by block number)

A finite element algorithm is described for computing steady and unsteady (oscillatory and transient) transonic flows over thin airfoils by solving directly the unsteady, nonlinear transonic potential equation based on small disturbance theory. The numerical algorithm is developed using the concept of finite elements in conjunction with the least squares method of weighted residuals applied to both space and time. The basic element presently used is a product of an element in space and an element in time. The former has a cubic expansion

over

DD FORM 1 JAN 73 1473 EDITION OF 1 NOV 65 IS OBSOLETE

UNCLASSIFIED

SECURITY CLASSIFICATION OF THIS PAGE (When Data Entered)

210105

AB

inside each element, while the latter is a quadratic Lagrange element. The embedded shocks are smeared and, in computing flow over lifting airfoils, use is made of the far field asymptotic solution to increase computational efficiency. For each time step, the finite element discretization in both space and time results in a recurrence relationship in the form of a banded system of algebraic equations, which is solved by Gaussian eliminations. Sample problems of steady flow over lifting airfoils and unsteady flow over airfoils executing harmonic motion are calculated to demonstrate the applicability and validity of the present approach. The solution procedures are found to be adequately accurate and very efficient, with unsteady solution obtainable in less than ten minutes CPU time on a CDC 6600 computer.

FOREWORD

This report was prepared by personnel in the Engineering Sciences Section of the Lockheed Missiles & Space Company, Inc., Huntsville Research & Engineering Center, Huntsville, Alabama, for the Air Force Flight Dynamics Laboratory, Wright-Patterson Air Force Base, Ohio. The computer programs were developed under Project 1370, "Dynamic Problems in Flight Vehicles," Task 137004, "Design Analysis," Contract F33615-75-C-3125. Capt. Gerald Van Keuren, AFFDL/FBR, is the Air Force Project Engineer.

S. T. K. Chan was the principal investigator for the study, and H. C. Chen, as co-investigator, contributed to the development of the numerical solution method and developed most of the necessary computer programs. The study was conducted under the supervision of M. R. Brashears and later B. H. Shirley.

The authors submitted this report in March 1976 as an AFFDL technical report to cover research performed from July 1975 to March 1976. This report contains the pertinent theory and numerical solution method, based on which a computer program was developed and documented as AFFDL/TR-76-49, Vol. II.

TABLE OF CONTENTS

LIST OF ILLUSTRATIONS

LIST OF ILLUSTRATIONS (Continued)

LIST OF SYMBOLS

Symbol	
a	local speed of sound
c	chord length of airfoil
C	constant indicating the type of the steady transonic equation
C_p	pressure coefficient
$g(x)$	airfoil geometry at mean position
h	function describing the airfoil oscillation about mean steady position
k	reduced frequency based on semi-chord
L_i	right-hand side vector of the resulting system of equations
$M = V/a$	local Mach number
M_∞	freestream Mach number
M_k	shape functions in time
N_i	shape functions in space
p	local static pressure
p_o	stagnation pressure
p_∞	freestream pressure
R	residual resulting from an approximate solution
S_1, S_2, S_3	boundary of flow field depicted in Fig. 2
S_{ij}	system coefficient matrix
T	period of oscillation
u, v	perturbed velocity components in the x- and y-directions, respectively
V	the flow speed
U_∞	freestream speed

LIST OF SYMBOLS (Continued)

Symbol	
$x = x'/c$ $y = y'/c$	nondimensional x and y coordinates
$t = t' \frac{U_\infty}{c}$	nondimensional time
Greek	
β	$\sqrt{1 - M_\infty^2}$
Γ	total circulation strength
γ	ratio of specific heats ($\gamma = 1.4$ for air)
ϵ	small number used as convergence criterion
δ	amplitude of the oscillating flap
$\phi = \phi'/(U_\infty \cdot c)$	nondimensional perturbation velocity potential
$\hat{\phi}$	approximate solution of ϕ
ϕ_i^k	undetermined parameter at nodal point i and time level k
χ	integral expression for the squared errors over the entire flow domain
∇	gradient of a scalar function
Superscripts	
+	upper surface of the airfoil or wake
-	lower surface of the airfoil or wake
k	time level k

Note: Subscripts after a comma indicate partial differentiations. In addition, a repeated index implies summation unless specified otherwise.

SECTION I
INTRODUCTION

In recent years, significant progress has been made toward developing a useful method for predicting steady transonic airloads over airfoils and to some degree for finite wings. Despite this progress, however, very few satisfactory methods exist for calculating unsteady transonic flows, as evidenced in a recent survey paper by Bland (Ref. 1). Only recently have numerical solutions via the finite difference relaxation techniques been presented for two-dimensional airfoils executing harmonic motion. As an alternative solution technique, the authors have recently investigated the application of the finite element technique for solution of the transonic flow problem, and computed successfully transonic flow over nonlifting thin airfoils (Ref. 2). Compared with the general finite difference relaxation techniques, the finite element method provides a more flexible mesh arrangement, element shape and size to cope more effectively with complex geometry and boundary conditions. Also, higher order approximations can be readily implemented to increase computational efficiency.

In the present study, the finite element technique is extended to compute lifting, unsteady transonic flows over airfoils. Since the objective of the present study is to develop an efficient and accurate numerical algorithm for the analysis of unsteady transonic flow over thin airfoils, the present formulation is therefore based on the small disturbance but nonlinear transonic potential equation for inviscid, compressible fluid. Unlike most existing techniques (Refs. 3 through 6) for solving the small disturbance potential equation, the present approach is aimed at solving directly the unsteady transonic equation, with both time derivative terms retained. Thus the present algorithm can be applied to compute a much wider class of transonic flow problems, including steady, oscillatory or transient solutions, either with or without angle of attack. For oscillatory flow, no assumption is made regarding the oscillating frequencies, nor must the unsteady perturbation be small compared to the mean steady solution.

On the numerical aspects, the present numerical algorithm is developed using the concept of finite elements in conjunction with the method of weighted residuals. However, to treat properly the mixed flow behavior, the residuals are modified by introducing a "one-sided assembly" scheme in the supersonic region. Also, a patching technique has been developed to match the finite element solution constructed in a moderately large domain with an asymptotic solution for the far field to avoid having to use a very large domain otherwise needed in computations. The basic element presently used is a product of an element in space and an element in time. The element in space has a cubic expansion inside the element, with nodal unknowns representing the perturbed velocity potential and the two perturbed velocity components; while the element in time is a quadratic Lagrange element. The resulting system of algebraic equations is banded, although nonsymmetric, which is solved conveniently by Gaussian elimination.

The computations of steady transonic flow over lifting airfoils are described in Section II, including relevant equations, the numerical approach and computed results. Considered in Section III are the calculations of unsteady transonic flow, which indeed can be applied also to compute steady transonic flow. The final section contains conclusions and recommendations for future studies.

SECTION II
STEADY TRANSONIC FLOW OVER LIFTING AIRFOILS

The small perturbation theory for steady transonic flow over lifting airfoils and the numerical approach for solving the nonlinear transonic equation are discussed in this section. First, the theory including the small perturbation potential equation with associated boundary conditions, together with related secondary unknowns, are summarized. A finite element algorithm based on a modified least squares method of weighted residuals is then described regarding the finite element formulation, special considerations of supersonic regions, the imposition of boundary conditions, and iterative procedures used to solve the resulting system of nonlinear algebraic equations. Finally, typical flow fields for a 6% thick circular arc and a NACA 64A 410 airfoil are computed to demonstrate the feasibility and applicability of the present approach.

1. ASSUMPTIONS AND BASIC EQUATIONS

Since the objective of the present study is to compute transonic flows over thin airfoils, small disturbance theory is generally adequate and hence used as the basis of this numerical model. With this theory, perturbation of the flow due to the presence of airfoils is assumed to be everywhere small, the embedded shock waves are assumed to be weak and boundary layer effects are neglected. Also, the flow is assumed to be isentropic and inviscid. These assumptions lead to a nonlinear equation of mixed elliptic-hyperbolic type for general two-dimensional steady transonic flow problems.

Differential Equation

$$\left[1 - M_\infty^2 - M_\infty^2 (1 + \gamma) \phi_{,x}\right] \phi_{,xx} + \phi_{,yy} = 0 \qquad (1)$$

Boundary Conditions

$$v - (1 + u)\frac{dg}{dx} = 0 \qquad \text{on the airfoil} \tag{2}$$

$$\nabla\phi = 0 \qquad \text{at infinity} \tag{3}$$

where ϕ = perturbed velocity potential function, u, v = perturbed velocity components in the x- and y-directions, respectively, M_∞ = freestream Mach number, γ = ratio of specific heats, taken to be 1.4 for air, and g = function of x defining the geometry of the airfoil including angle of attack. Equation (1) is in dimensionless form and the x-axis is aligned with the undisturbed flow direction. The dimensional (with primes) and nondimensional quantities are related by

$$x = \frac{x'}{c}, \quad y = \frac{y'}{c} \quad \text{and} \quad \phi = \frac{\phi'}{U_\infty c}$$

where c and U_∞ are the characteristic length and speed, which are currently taken as the chord length and the freestream speed, respectively.

For flow over lifting airfoils, due to the presence of circulation, the velocity potential function is not continuous but possesses a jump equal to the circulation strength. For this reason, a branch cut must be made to allow the potential function to acquire a jump, but with continuous velocities. Therefore, along a branch cut, the following conditions must be imposed.

$$\begin{aligned} \phi^+ - \phi^- &= \Gamma \\ u^+ - u^- &= 0 \\ v^+ - v^- &= 0 \end{aligned} \tag{4}$$

in which "+" and "-" designate the upper and lower surfaces of the branch cut, and Γ represents the strength of circulation.

Once the flowfield solution in terms of the perturbed velocity potential has been obtained, all secondary unknowns can then be calculated. These include

$$a = \left[\frac{\gamma-1}{2}\left(U_\infty^2 - V^2\right) + \left(\frac{U_\infty}{M_\infty}\right)^2\right]^{1/2} \tag{5}$$

$$M = \frac{V}{a} \tag{6}$$

$$\frac{p}{p_o} = \frac{1}{\left[1 + \frac{\gamma-1}{2} M^2\right]^{\gamma/\gamma-1}} \tag{7}$$

$$C_p = -\left[\frac{2u}{U_\infty} + (1 - M_\infty^2)\frac{u^2}{U_\infty^2} + \frac{u^2}{U_\infty^2}\right] \cong -\frac{2u}{U_\infty} \tag{8}$$

In the above, $U_\infty = 1$, the normalized freestream speed, a = local speed of sound, M = local Mach number, V = the flow speed, p = local static pressure, p_o = stagnation pressure, and C_p = pressure coefficient.

2. NUMERICAL APPROACH

The finite element method, in conjunction with the least squares method of weighted residuals, is used herein to solve numerically the small perturbation transonic equation. Summarized in this subsection are the finite element formulation, considerations of the embedded supersonic regions, imposition of boundary conditions, and finally iterative procedures used to solve the resulting system of nonlinear algebraic equations. The present numerical approach is a direct extension of a previous study for transonic flow over nonlifting airfoils. More detailed discussion is given in Ref. 7.

Finite Element Formulation

To solve the present problem by finite element methods in conjunction with the least squares approach, a set of locally defined trial functions with undetermined parameters is first assumed as the approximate solution, and the integral expression for the square of errors committed by the approximate solution is formulated. Then the integral of square errors in the entire domain is minimized with respect to the undetermined parameters to yield a system of algebraic equations. In actual computations, the minimization process is performed at element level and then an assembling process is invoked to obtain the system of algebraic equations.

Written in the usual manner with repeated indices implying summation, the approximate solution has the following form

$$\hat{\phi} = N_i \phi_i \tag{9}$$

in which N_i's represent the shape functions and ϕ_i's are the undetermined parameters at nodal points. The residual then becomes

$$R = \left\{ \left[1 - M_\infty^2 - M_\infty^2 (1 + \gamma) N_{k,x} \phi_k \right] N_{j,xx} + N_{j,yy} \right\} \phi_j \tag{10}$$

from which an integral expression for the square errors is obtained as

$$\chi = \iint R^2 dA \tag{11}$$

Upon the minimization of χ with respect to the undetermined parameters, a system of algebraic equations in the following form is obtained

$$S_{ij} \phi_j = 0 \tag{12}$$

Herein the banded system matrix S_{ij} is defined as

$$S_{ij} = \iint P_i \, Q_j \, dA \tag{13}$$

with P_i and Q_j defined by the following expressions

$$Q_j = \left[1 - M_\infty^2 - M_\infty^2 \, (1+\gamma) \, N_{k,x} \, \phi_k \right] N_{j,xx} + N_{j,yy} \tag{14}$$

and

$$P_i = Q_i - M_\infty^2 \, (1+\gamma) N_{k,xx} \, \phi_k \, N_{i,x} \tag{15}$$

As stated earlier, the system matrix is obtained by combining appropriate contributions from all the elements. The element matrices, in turn, are evaluated effectively by numerical integration to avoid the tedious and error prone algebraic manipulations. It is to be noted that although the system of equations, Eq. (12), is homogeneous, it does possess a non-trivial solution once the boundary conditions are imposed.

The basic element used in the present program is the nonconforming cubic triangular element developed by Bazeley et al. (Ref. 8). Also used in the program are quadrilateral and trapezoidal elements constructed from these triangular elements. These three types of elements can be mixed and used freely in the entire flow region except that only trapezoids should be used to cover adequately the supersonic region in order to enact the special treatment discussed later.

The basic triangular element is shown in Fig. 1, which at each vertex has the function itself and its two first derivatives (velocity components) as undetermined parameters. This type of element was adapted mainly because boundary conditions of both Dirichlet and Neumann types can be imposed with equal convenience. In addition, because velocities at nodes are treated as primary unknowns, secondary unknowns such as local Mach number, and

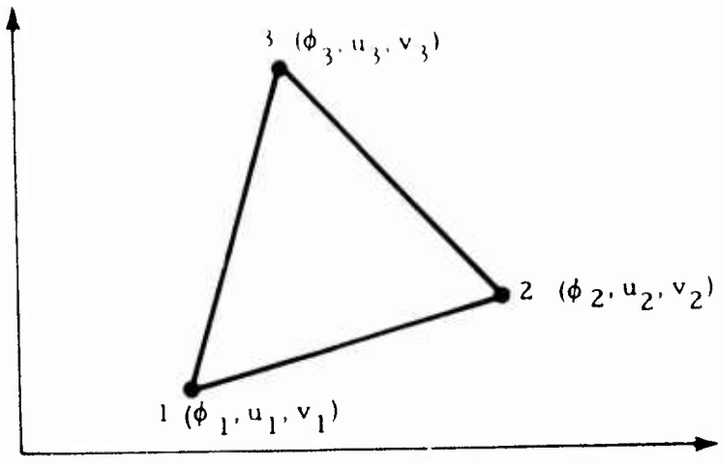

Figure 1 - Triangular Element with Undetermined Parameters

pressure coefficients, etc., can be computed directly without resorting to numerical differentiation, thus assuring higher accuracy. Furthermore, the use of higher order elements can usually improve computational efficiency as evidenced in most finite element analyses.

As is known, the elements presently used are C^1 continuous only at nodal points but not across element boundaries, which apparently violates C^1 continuity between elements as normally required. However, our experience as well as applications by others do not seem to indicate that such a requirement is necessary, though it is obviously a sufficient condition for monotonic convergence as the element mesh is refined. For the problems of plate bending, it was concluded that the condition necessary to guarantee convergence is that the element used should be capable of representing constant curvatures (second derivatives) within the element, as evidenced by several cases of plate bending analysis (Ref. 8). The inter-element continuity requirement for solving the present second order equation using least squares should be the same as that for solving a fourth order equation using the variational principle, as the integral forms for both problems involve up to second derivatives only. In the present study, use has been made of these simpler

"non-conforming" elements and results appear to be adequately accurate. It is to be emphasized that "conforming" elements (with continuous normal derivatives between elements) do exist and can be readily implemented. With these elements, however, more sophisticated techniques for handling the discontinuity along the path of shock wave may also become more desirable. Some studies on the effects of "non-conforming" versus "conforming" elements, together with more sophisticated schemes for handling shocks, are indeed highly desirable and useful.

Considerations of Supersonic Regions

As is well known, the finite element method is a powerful tool for solving problems governed by elliptic equations. However, for problems governed by either parabolic or hyperbolic equations, the conventional finite element assembly technique must be modified so that the proper influence of solution in time (or time-like direction) is considered. For the present problem, the x-axis is the time-like direction which implies that the solution at the upwind station will determine the solution at its downwind station but not the contrary. This consideration leads to the well known upwind influence finite difference operator (backward finite difference). An equivalent technique in finite element analysis has been devised and applied to solve the transonic flow equation.

Consider the rectangular element sketched below with upwind station I and downwind station II, each having two nodal points. With the element type chosen, the element matrices can be constructed in the usual manner. However, before assembling the element matrices into the system matrix, the coefficient of the

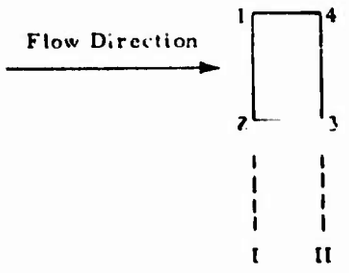

first term in the transonic equation should be evaluated

$$C = 1 - M_\infty^2 - M_\infty^2 (1 + \gamma) u \tag{16}$$

The sign of the coefficient C being positive, zero, or negative will define the equation as elliptic, parabolic or hyperbolic. If C is non-positive for all nodes in the element, the rows representing the improper downwind influence on the solution at an upwind station are ignored during assembly. This feature is taken care of automatically in the program, requiring only a little care with the nodal arrangement in the element. In the anticipated supersonic region, element node points should be arranged in the order as indicated in the above sketch, starting with the upper left corner node and proceeding in a counter-clockwise direction. On the other hand, if the sign of C is positive at any of the four nodes, no special assembling is invoked. As stated earlier, only trapezoidal elements are to be used in the anticipated supersonic and mixed flow region, while triangular elements and quadrilaterals consisting of only two triangles are considered unsuitable because of their bias nature. However, these two latter types of elements can be used effectively in the subsonic flow region.

Imposition of Boundary Conditions

As stated earlier, the imposition of boundary conditions for the present problem can be carried out conveniently because the elements presently used have the function value and the two first derivatives as primary unknowns. The associated boundary conditions thus can be treated as the essential type, i.e., having prescribed values. Standard finite element methodology is therefore followed by assembling first an unconstrained problem and then modifying the matrix equations accordingly.

On the airfoil, the nonlinear form of flow tangency on the airfoil is imposed by replacing the algebraic equation for v_i by

$$v_i - \frac{dg}{dx} u_i = \frac{dg}{dx} \tag{17}$$

in which u_i and v_i are unknown parameters at node "i" on the airfoil. When the linear form is desired, the corresponding equation becomes

$$v_i = \frac{dg}{dx} \tag{18}$$

and is applied along the chordline.

For the far field boundary condition, Eq. (3) is valid only at infinity, and thus an infinite domain is required in computations if the condition is to be imposed directly. Although an approximation can be made by assuming Eq. (3) to be valid on a boundary at a finite distance from the airfoil, a large computational network is usually required to obtain a solution with adequate accuracy due to the fact that for lifting airfoils at transonic speeds, the disturbances created by the body decay very slowly. There are several ways to cope with this problem so that computations can be restricted to a finite region. One approach is to map the region exterior to the airfoil into the interior of a circle upon which the computations are performed and the final solution is obtained by a subsequent inversion (Ref. 9). This technique is almost ideal for computations involving a single airoil, but its extension to three-dimensional cases or flow over multiple airfoils is not evident. Another approach is to match the numerical solution of the near field with an analytic representation for the far field to satisfy, in effect, the far field boundary conditions, as employed in finite difference relaxation techniques (Refs. 10 and 11). In doing so, computations can be performed in the physical plane by using a finite domain without sacrificing too much accuracy and more importantly, it provides a straightforward extension to treat three-dimensional and multiple airfoil problems. This concept is pursued with appropriate modifications in the present finite element solution technique so that the circulation and hence lifting force is computed by a systematic approach.

Figure 2 depicts a lifting airfoil under free-flight conditions. In the analysis, a moderately large domain, R', is taken to construct the finite element solution, while an asymptotic solution with undetermined parameters

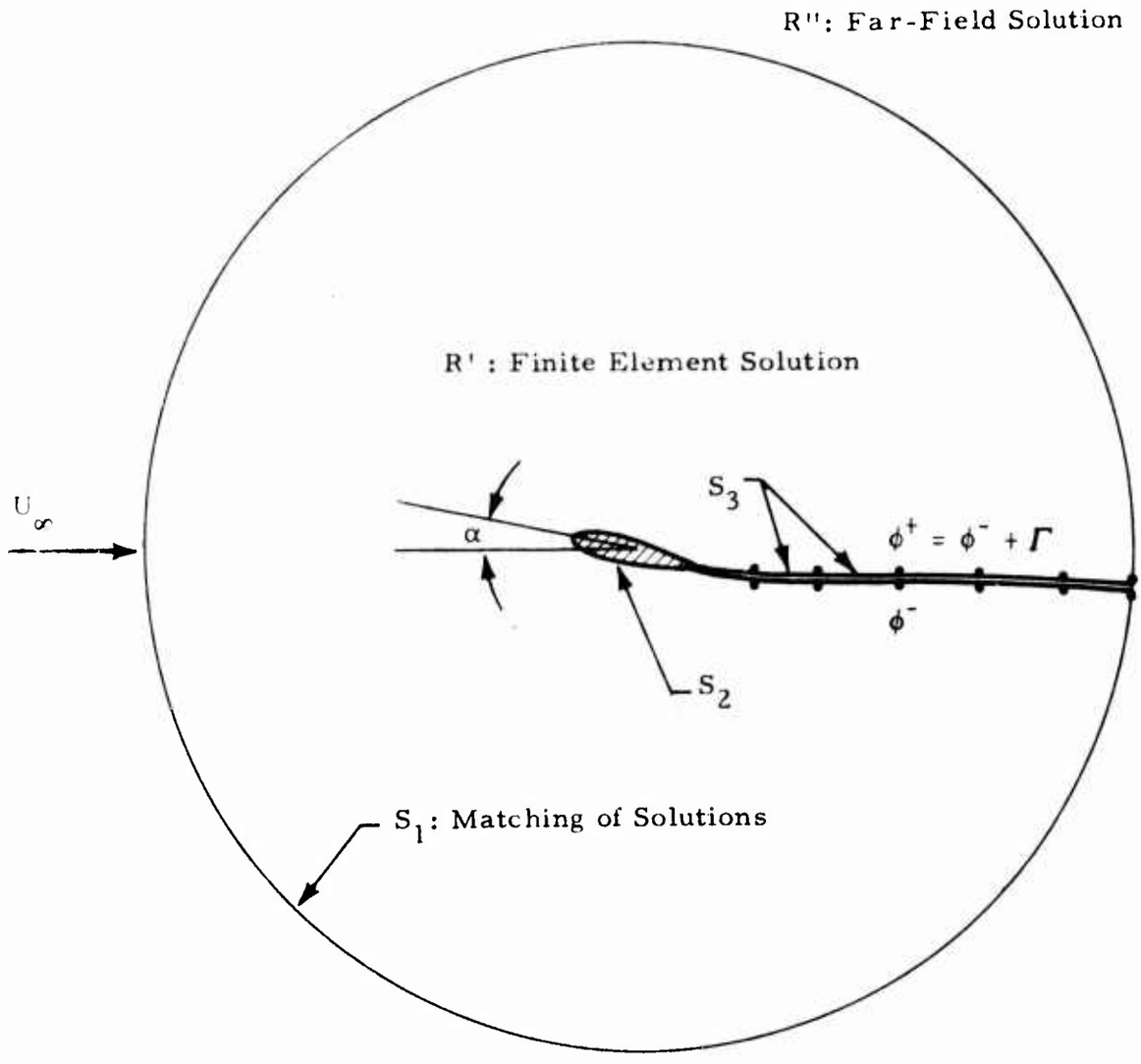

Figure 2 - Matching of Localized Finite Element Solution with Far-Field Solution

is assumed to be valid in the far field, R''. The two solutions are then matched along the common boundary, S_1, along which the unknowns are then expressed in terms of the far-field undetermined parameters. Along the branch cut, S_3, the conditions of the velocity being continuous but the velocity potential possessing a jump equal to the circulation, Γ, are imposed iteratively. Through these procedures, the far-field parameters will be determined systematically rather than merely by trial and error.

The far-field potentials for both lifting airfoils and three-dimensional wings at transonic speeds were developed by Klunker (Ref. 12). The expression for a two-dimensional airfoil is currently used and has the following form

$$\phi = \frac{\Gamma}{2\pi}\left[\frac{\pi}{2}\,\mathrm{sgn}\,(y) + \tan^{-1}\left(\frac{x}{\beta y}\right)\right]$$

$$+ \frac{1}{\pi\beta}\,\frac{x}{x^2 + \beta^2 y^2}\int_C g(\xi)\,d\xi \qquad (19)$$

$$+ \frac{M_\infty^2\,(1+\gamma)}{4\pi\beta}\int_A u^2\,\frac{(x-\xi)}{(x-\xi)^2 + \beta^2\,(y-\eta)^2}\,dA$$

The first term on the right-hand side corresponds to a free vortex and represents the lifting effects; the second term corresponds to a source distribution whose strength is related to the airfoil geometry g(x); and the third term, which arises from the nonlinearity of the flow equations, has the form of a doublet with its strength given by the local value of u^2 and is to be integrated over the flow domain under consideration. Klunker also showed that the contributions from the thickness and the area integrals are of higher order effects. For these reasons, only the first term representing the lifting effects is used currently for the far field. The solution along the outer boundary S_1 is updated systematically, using the computed potential jump at the trailing edge.

The boundary condition, Eq. (4), along the branch cut can be considered as constraints to the unknown parameters. These constraints can be imposed through introducing Lagrangian multipliers. As an alternative, a scheme without the need of introducing Lagrangian multipliers was devised and implemented. The scheme is essentially based on the concept of using chain rule in minimizing the integral of square errors. More specifically, the algebraic equations are first generated assuming no constraint on the original parameters. However, because of constraint on certain unknown parameters, the algebraic equations corresponding to constrained parameters are then manipulated according to chain rule and the specific constraint to yield one equation less for each constraint. And finally, one unknown parameter could be eliminated for each constraint, thus making the total number of equations and unknowns equal. A variation of this scheme is to insert, in place of the equation eliminated, the constraint and leave the total number of unknown parameters unchanged. The latter approach has the advantage of simpler bookkeeping and was therefore implemented in the computer program. For example, to impose the condition $u^+ = u^-$ for a pair of nodes along the branch cut, the equation originally generated for u^- is first added to the equation for u^+, and then in its place the constraint equation $u^+ - u^- = 0$ is inserted.

Iterative Procedures

With the equations properly assembled and boundary conditions imposed, the system of nonlinear algebraic equations is finally solved by iterative procedures of the form

$$S_{ij}(\bar{\phi})\,\phi_j^{(n)} = L_i \tag{20}$$

to solve for the solution $\phi^{(n)}$ at the n^{th} iteration. The function $\bar{\phi}$ is, in turn, defined as

$$\bar{\phi} = \theta\,\phi^{(n-1)} + (1 - \theta)\,\bar{\phi}^{(n-1)} \tag{21}$$

in which θ is a relaxation factor in the range $0 < \theta \leq 1$. For subsonic flow, θ is usually taken as unity; for flow in the transonic regime, however, it has been found that the use of an under-relaxation factor is required. The value of θ should decrease from unity for barely critical flow to 0.4 or even 0.3 for supercritical flow. The optimum under-relaxation factor generally depends on the freestream Mach number and the mesh being used. At the present, no systematic investigations have been done in this regard, and therefore its value should be selected by numerical experimentations. Generally speaking, a smaller under-relaxation factor will make the solution more stable but at the same time tends to slow the rate of convergence.

Equation (20) is to be solved subject to certain prescribed convergence criteria. The one presently used is that the relative change of local Mach number between two consecutive iterations should be less than a prescribed small number for all the nodes in the flow field, that is

$$\left| \frac{M^{(n)} - M^{(n-1)}}{M^{(n)}} \right| < \epsilon \tag{22}$$

The value of ϵ in most numerical computations is in the range $0.001 \leq \epsilon \leq 0.005$.

The numerical procedures can thus be summarized as the following:

1. Construct finite element algebraic equations for the inner field based on the method of weighted residuals, presently with the least squares approach with modifications made in supersonic regions.
2. Apply boundary condition on the airfoil to satisfy flow tangency condition at nodal points.
3. Impose the continuity of velocity components along the branch cut as described earlier.
4. Specify the parameters along the common boundary of inner and outer field in terms of the value of circulation strength.

5. Solve for the flow field and hence the jump in potential at the trailing edge, which is then used as an improved solution in updating the finite element algebraic equations and the circulation along the outer boundary, respectively.

6. Repeat the above procedures until a convergent solution is obtained, such as until the relative change of Mach number falls within a small range of tolerance or the jump in potential function across the branch cut is essentially a constant.

3. NUMERICAL RESULTS

To demonstrate the applicability of the present approach, flow fields over a 6% thick circular arc and a NACA 64 A410 airfoil have been computed. Results obtained by the present approach appear to compare, in general, very well with experimental data and those obtained by relaxation techniques, while each case calculated requires only a few minutes of CPU time on a Univac 1108 computer.

For the 6% thick circular arc, calculations were made for cases with angle of attack equal to 1 and 2 deg. The mesh presently used is shown in Fig. 3, with 202 nodes. As is seen in the figure, the mesh arrangement is completely flexible, except in the expected supersonic region where a rather regular mesh is needed in order to consider properly the problem of region of dependence. The predicted results for the two cases are shown in Figs. 4 and 5, respectively, where comparisons are made with experimental data obtained by Knechtel (Ref. 13). It is seen that the agreement between the predicted results and experimental data is excellent except near the leading and trailing edges. These noticeable discrepancies are believed mainly due to the invalidity of the small perturbation equation in these regions. In addition, the present computations are based on inviscid theory, while experimental results necessarily involve viscous effect, which were evidenced in the form of negative aerodynamic loadings over the rear portion of the airfoil. For these reasons, the predicted results are considered to be sufficiently accurate. Among all of the cases calculated, the greatest difference appears

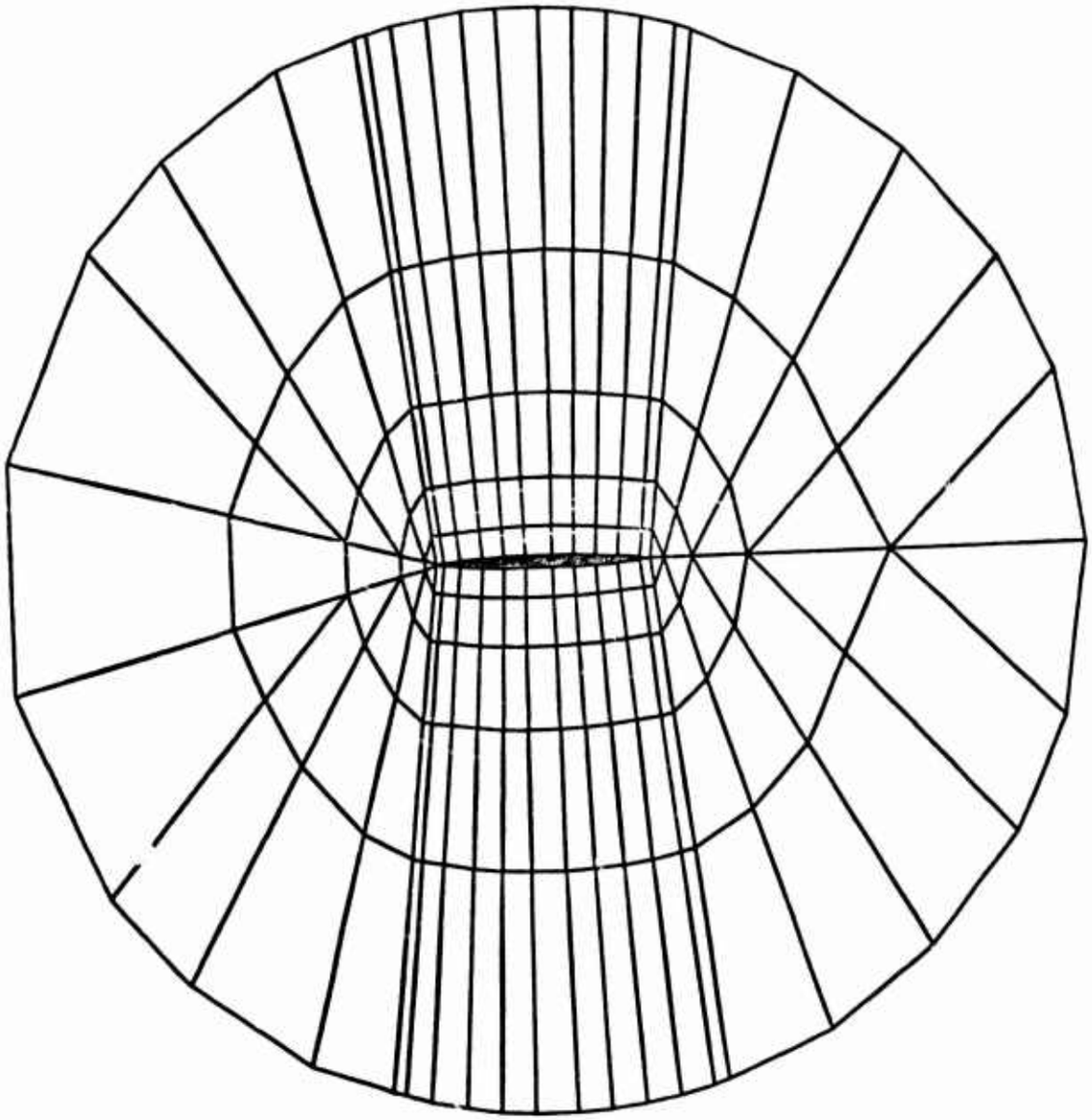

Figure 3 - Finite Element Mesh Layout (173 Elements, 202 Nodes)

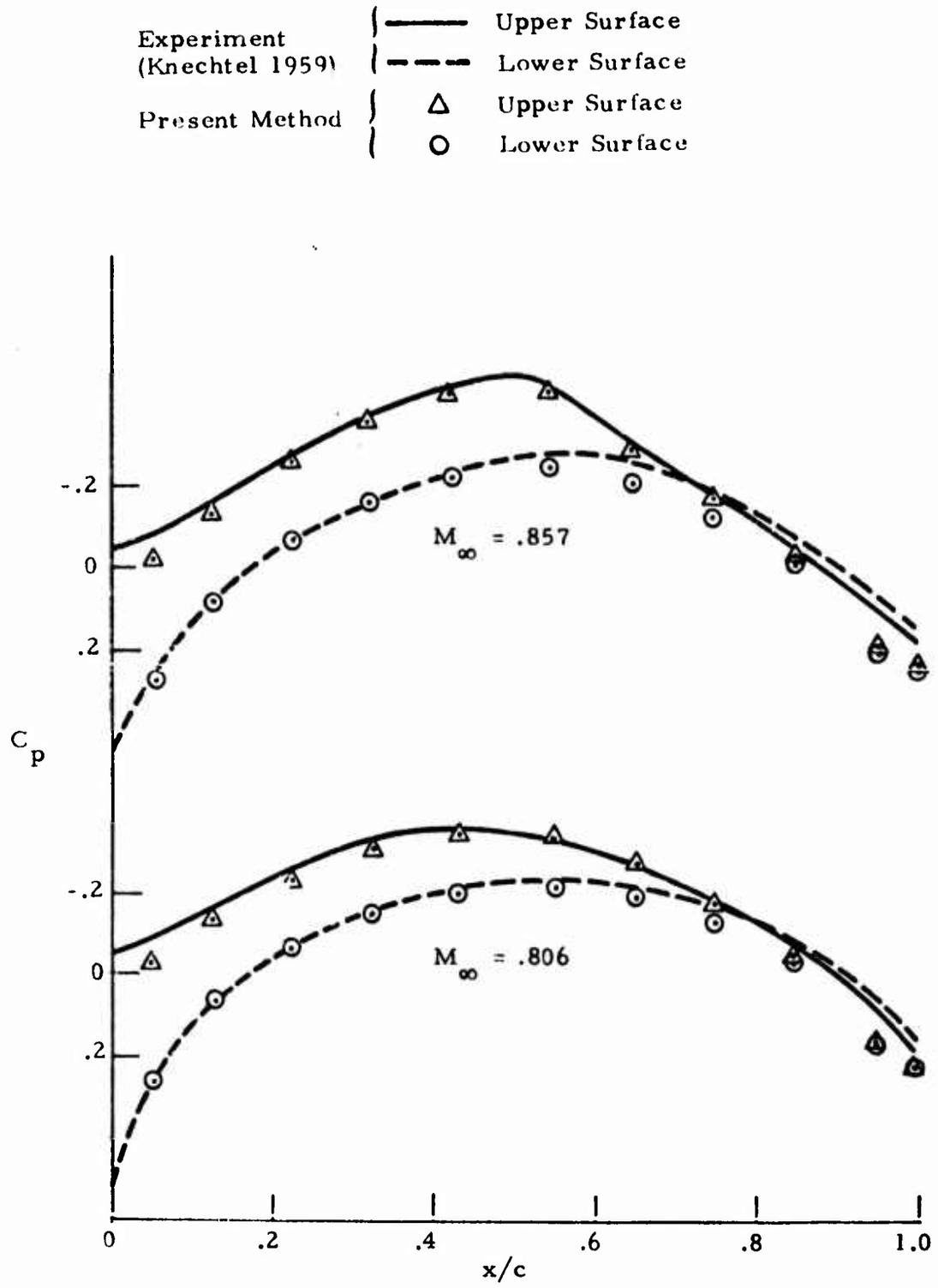

Figure 4 - Comparison of Chordwise Pressure Distribution for a 6% Thick Circular-Arc Airfoil (α = 1 deg)

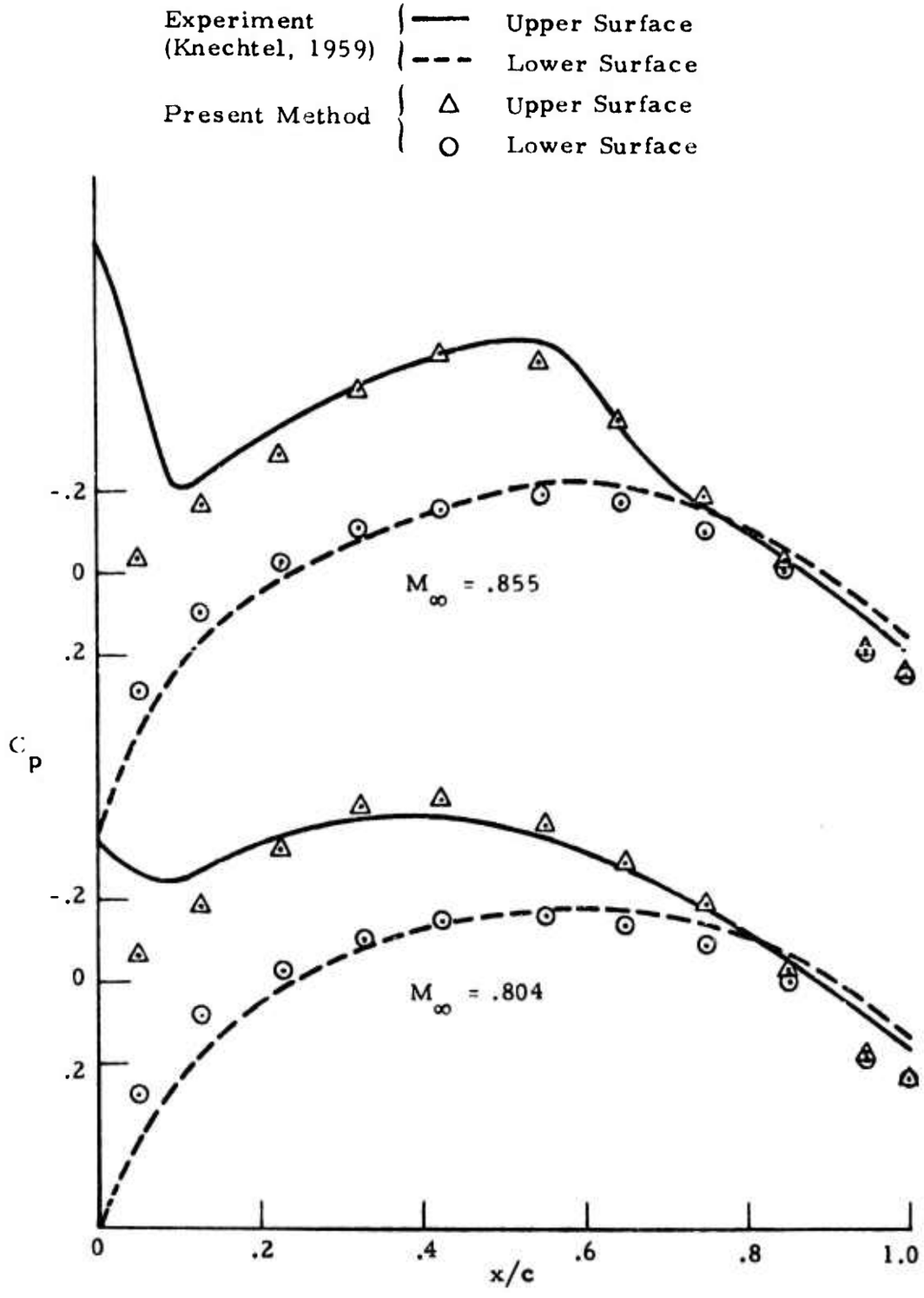

Figure 5 - Comparison of Chordwise Pressure Distribution for a 6% Thick Circular-Arc Airfoil (α = 2 deg)

to be near the leading edge for the critical case ($\alpha = 2^{o}$, $M_{\infty} = 0.855$), where a large peak pressure is present in the experiment. However, as other cases of lower and higher Mach numbers do not indicate such large peak pressure near the leading edge (see Fig. 7e of Ref. 13), the peaky behavior for the present case is somewhat peculiar and questionable.

To test the present approach further, the flow field over a NACA 64 A410 airfoil was also computed. This airfoil was chosen as another testing case mainly for two reasons: (1) the airfoil is thicker (with 10% thickness ratio) and blunt-nosed, thus it represents a more severe test for the present method; and (2) the airfoil has been studied rather extensively and both experimental and numerical data are available for comparisons (see Ref. 11). To date, only limited computations have been performed. Preliminary results are depicted in Figs. 6, 7 and 8 for cases involving various Mach numbers, either with or without angle of attack. As the present airfoil has a blunt leading edge, the boundary condition in that region cannot be imposed in the usual manner by specifying the vertical velocity component as $v = dg/dx = \infty$. Several numerical experiments have been conducted to cope with these difficulties. One of the attempts is to specify the normal derivative of the perturbed velocity potential. The value of the normal derivative, in turn, can be determined explicitly from the flow tangency condition. To accomplish this in the numerical computations, the normal and tangential derivatives of the potential function are used as unknowns at the leading edge, instead of the derivatives originally in the x- and y-directions. Thus the normal derivative of the perturbation potential can be conveniently specified. These thoughts have been implemented into the program. However, our numerical experimentation indicates that the imposition of a full amount of perturbed normal velocity as computed from flow tangency condition (without invoking the small perturbation assumption) does not produce satisfactory results near the leading edge, with the flow in that region being impeded excessibly. The inaccuracy of the solution in this region is believed partly due to the mesh being

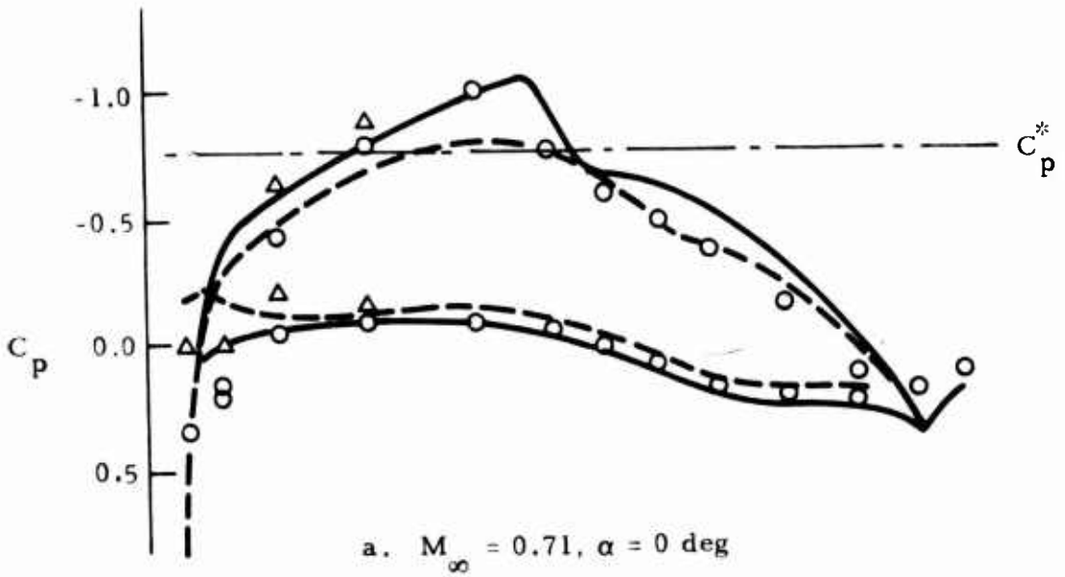

a. $M_\infty = 0.71$, $\alpha = 0$ deg

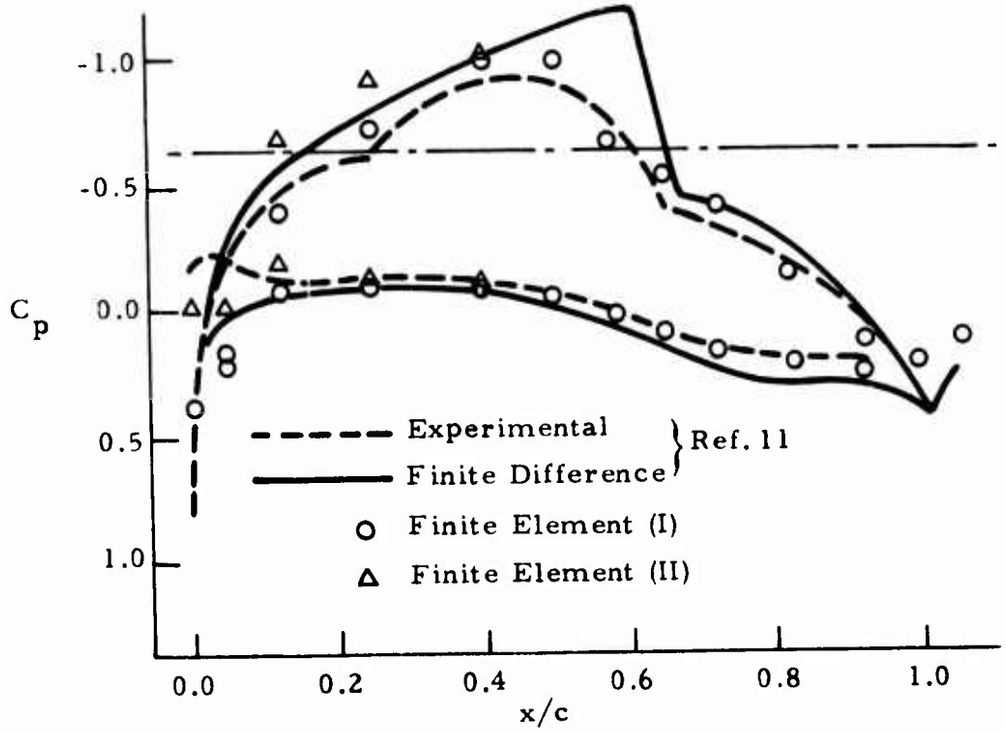

b. $M_\infty = 0.74$, $\alpha = 0$ deg

Figure 6 - Comparison of Chordwise Pressure Distribution for NACA 64 A410 Airfoil ($\alpha = 0$ deg)

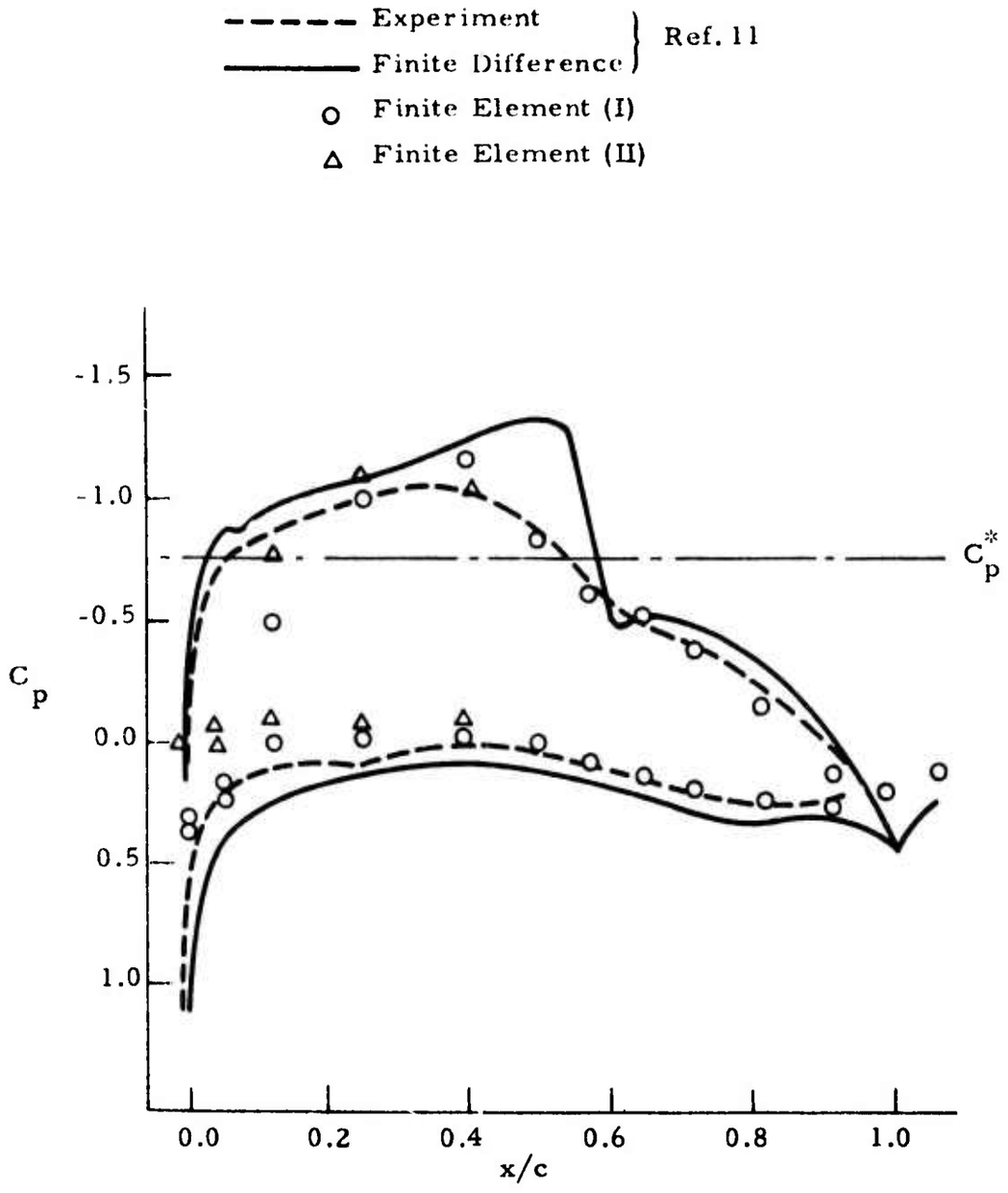

Figure 7 - Comparison of Chordwise Pressure Distribution for NACA 64 A410 Airfoil (M_∞ = 0.70, α = 2 deg)

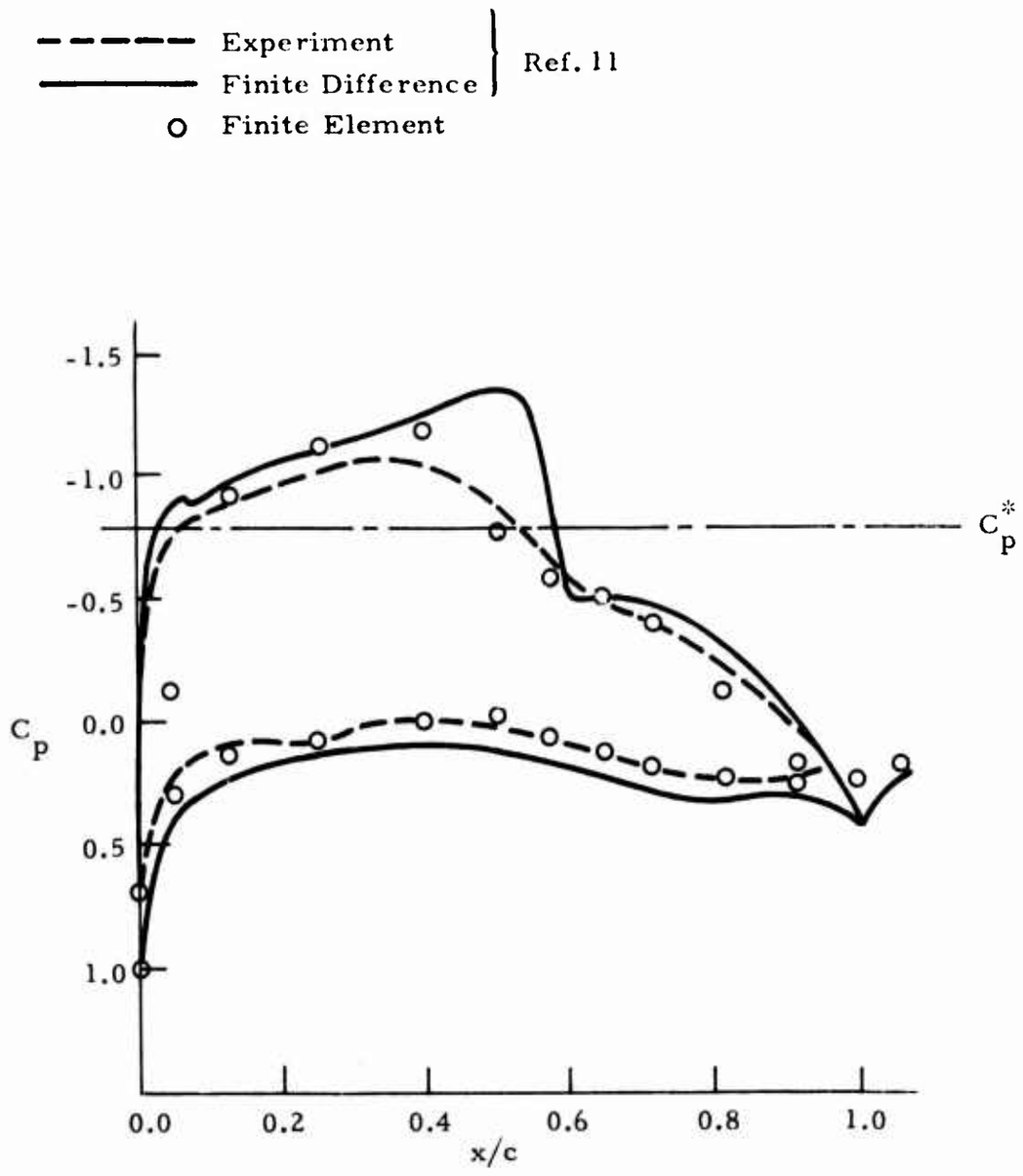

Figure 8 - Comparison of Chordwise Pressure Distribution for NACA 64 A410 Airfoil (M_∞ = 0.70, α = 2 deg) by Specifying Finite Slopes at the Leading Edge

too coarse and partly due to the fact that the boundary condition used does not match the small disturbance equation there. In an attempt to make the boundary condition at the leading edge compatible with the small perturbation equation which is assumed to be valid there, numerical experimentations were performed by specifying only a fraction of the perturbed velocity in the normal direction, with results depicted in Figs. 6 and 7. Method I corresponds to one-fourth of the normal velocity otherwise required, while Method II has a zero normal perturbed velocity specified. As is seen, the pressure distribution near the leading edge is quite sensitive to the boundary condition imposed there; however, the comparison for the remaining portion of the airfoil is very good. Another attempt is to use finite values of slope for the nodal points at the leading edge and impose the flow tangency condition as required by Eq. (17). Figure 8 presents results obtained by using at the leading edge half the value of the airfoil slopes at 0.5%. Compared with the predicted results shown in Fig. 7, some improvement near the leading edge is apparent, but the expansion on the upper surface is still not properly simulated. Nevertheless, as seen in the figures the inaccuracy near the leading edge is localized and is always confined to the first few nodal points. The solution accuracy could be improved within the small disturbance assumption to a certain extent by refining the mesh near the leading edge. However, because the core storage capacity normally available on the local Univac 1108 computer is only 64K, some additional programming effort is required in order to compute the problem with a much finer mesh; therefore, only results with the present mesh are presented.

SECTION III
UNSTEADY TRANSONIC FLOW

In this section, finite element procedures are described for solving the problems of unsteady transonic flow. Again, the formulation is based on small perturbation theory. However, unlike the approach developed earlier for NASA-Langley (Ref. 6), the assumptions of harmonic motion and the un steady disturbance being small compared to the mean steady solution are removed in the present approach. The removal of these assumptions allows the flow field to be computed in a wider range. These include the problems involving transient solution, moderate unsteadiness and, more importantly, movement of shock wave location. The equations, upon which the present numerical procedures are constructed, are summarized in Subsection 1. Two numerical approaches, namely, the Galerkin type and least squares method, which have been investigated to integrate directly the unsteady transonic equation, are described in Subsection 2. As a result of the present investigation, the Galerkin method of weighted residuals was found to be invalid for computing supercritical flow, thus the least squares approach has been pursued. To date, only limited computations have been conducted using the least squares approach; however, results obtained thus far indicate the present approach is, in general, very satisfactory. Typical results are summarized and discussed in Subsection 3.

1. BASIC EQUATIONS

Based on small perturbation theory, the unsteady transonic flow problem can be stated as

$$L(\phi) = \alpha\phi_{,xx} + \phi_{,yy} - 2M_\infty^2 \phi_{,xt} - M_\infty^2 \phi_{,tt} = 0 \qquad (23)$$

in which

$$\alpha = a + b\,\phi_{,x}$$

with

$$a = 1 - M_\infty^2$$

$$b = -M_\infty^2 (1 + \gamma)$$

The boundary conditions associated with Eq. (23) include:

- Vanishing of Disturbance at the Far Field,

$$\nabla\phi = 0 \tag{24}$$

- Flow Tangency Condition on the Airfoil Surface,

$$\frac{DB}{Dt} = B_{,t} + (1+\phi_{,x}) B_{,x} + \phi_{,y} B_{,y} = 0$$

with B describing the instantaneous airfoil position as

$$B(x, y, t) = y - g(x) - \delta h(x, t) = 0$$

In the above, g(x) = geometry of the airfoil at mean steady position, δ = amplitude of oscillation, and h(x, t) = function describing the airfoil oscillation. Upon substitution, a nonlinear boundary condition is obtained as

$$\phi_{,y} = \delta(h_{,x} + h_{,t}) + g_{,x} (1 + \phi_{,x}) \tag{25}$$

Which is to be imposed on the mean position of the oscillating airfoil, i.e., $B(x, y, t_{mean}) = 0$.

- Unsteady Kutta Condition in the Wake

Along the wake, pressures and downwashes are equal on both sides of the vortex sheet. Since the pressure coefficient is given, to the lowest order, as

$$C_p = -2\phi_{,t} - 2\phi_{,x} - \phi_{,y}^2$$

the linearized boundary conditions in the wake thus become

$$\phi^{+}_{,t} + \phi^{+}_{,x} = \phi^{-}_{,t} + \phi^{-}_{,x} \tag{26}$$

and

$$\phi^{+}_{,y} = \phi^{-}_{,y} \tag{27}$$

which are to be applied along the upper and lower surfaces of the mean wake position. The potential values on the upper and lower surfaces of the wake are related by

$$\phi^{+} = \phi^{-} + \Gamma \tag{28}$$

in which $\Gamma = \Gamma(x,t)$ for unsteady flows. With Γ as the primary unknown, the condition expressed by Eq. (26) can also be written as

$$\Gamma_{,t} = -\Gamma_{,x} \tag{26a}$$

As discussed earlier, for lifting airfoil computations, the far field conditions must be considered properly. To do this an asymptotic expression with undetermined parameters must be established and matched with the near-field finite element solution. In the present study, only the asymptotic solution for mean steady flow has been established and implemented, implying that the unsteady perturbation at far field is small compared to the mean steady solution.

2. NUMERICAL APPROACHES

The finite element technique, in conjunction with the Method of Weighted Residuals (MWR), is used to solve Eq. (23) with its associated boundary conditions. The approaches undertaken include the Galerkin type and the least squares method. At this stage, results indicate that the Galerkin approach can be used to compute flow in the subcritical regime but does not seem to be valid for calculating critical transonic flows. The least squares approach,

on the other hand, appears to be satisfactory when critical flow is considered. These two approaches are described in the following.

The Galerkin Approach

The Galerkin approach was investigated during the earlier stage of this study as it can offer certain advantages over the least squares formulation, especially when the unsteady transonic equation is considered. These include:

1. The formulation by Galerkin criterion is noticeably simpler and will require less computation time.
2. With appropriate integration by parts and arrangement, the continuity requirement between elements can be lowered and boundary conditions can be treated more conveniently.

With the Galerkin approach, an approximate solution for the velocity potential is first assumed in the form

$$\phi = N_i(x, y)\, \phi_i(t) \qquad (i = 1 \text{ to } n) \tag{29}$$

in which N_i = shape functions, ϕ_i = the corresponding undetermined parameters, and n = total number of unknown parameters. Equation (29) is then substituted into (23) and, with N_i as weighting functions, the procedure of weighted residuals is applied in the spatial directions to obtain a system of Ordinary Differential Equations (ODE) in the form

$$A_{ij}\, \ddot{\phi}_j + B_{ij}\, \dot{\phi}_j + C_{ij}\, \phi_j = 0 \tag{30}$$

in which the coefficient matrices are banded and are functions of space only.

To integrate Eq. (30), a Galerkin type time marching scheme is used to obtain a recurrence relationship which is implicit in nature. For instance, with a quadratic expression for the time history of each nodal unknown one has

$$\phi_j = M_k(t)\, \phi_j^k \qquad (k = 1 \text{ to } 3) \tag{31}$$

in which M_k represents the shape functions in time. Again, direct substitution and applying the method of weighted residuals (choosing M_3 as the weighting function) with integration carried out in time will result in a recurrence equation in the form

$$(a_k A_{ij} + b_k B_{ij} + c_k C_{ij}) \phi_j^k = 0 \tag{32}$$

where the vectors a_k, b_k, c_k are functions of time only. Equation (32) can be rewritten as

$$(a_3 A_{ij} + b_3 B_{ij} + c_3 C_{ij}) \phi_j^3 = -(a_m A_{ij} + b_m A_{ij} + c_m C_{ij}) \phi_j^m \tag{33}$$

$$(m = 1 \text{ to } 2)$$

From Eq. (33), the solution at time level k = 3 can be computed from solutions at the previous time steps. This process will continue until the solution sought is obtained.

A program based on the above formulation has been developed and used first to solve a steady problem which is obtained as the limiting flow for large times with suitable initial conditions. Presently the initial conditions are obtained by placing a leaky profile in the desired uniform stream and then impulsively turn off the leakiness at zero time. That is, the flow is assumed to be uniform for $t \leq 0$, and is required to satisfy the tangential boundary condition on the airfoil for $t > 0$. With a 6% thick circular arc airfoil, convergent results are obtained for $M_\infty = 0.806$ (subcritical) and $M_\infty = 0.84$ (barely critical). However, as M_∞ increases to 0.86 (critical), the sequence of unsteady flows oscillates from one time step to another and diverges. This phenomenon persists whether the improper downwind influence is removed or not.

In attempting to resolve the above problem, several numerical experiments (variations of the Galerkin approach) were then carried out for the steady transonic equation.

As found previously (Ref. 2) the transonic equation should not be cast into an equation of the Poisson type and treated as an elliptic problem. Any numerical scheme so constructed would inhere in it the improper downwind influence upon upwind solution in the supersonic region. To eliminate this, it is more convenient to apply the Galerkin approach directly without integration by parts for the term involving $\phi_{,xx}$. However, in order to obtain a better conditioned coefficient matrix, integration by parts for the $\phi_{,yy}$ term is carried out. This approach was also found unsuccessful in obtaining a convergent solution for the case $M_\infty = 0.861$.

Another attempt was to add a term simulating numerical viscosity for elements in the supersonic region. The term added is

$$\alpha \Delta X \phi_{,xxx} \tag{34}$$

In the finite difference approach, ΔX is the spacing between two grid points. When the transonic equation is discretized by a second order central difference formula, this term is capable of eliminating the downwind influence (Ref. 14). In our formulation, ΔX is taken to be the X dimension of the element. Again, no satisfactory results were obtained for the case of $M_\infty = 0.861$.

Other possibilities for modifying the conventional Galerkin approach to solve the transonic equation remain to be exploited. However, work in that direction could be time consuming and expensive. Based on its success with solving the steady transonic problem, the least squares approach was therefore investigated to solve also the unsteady transonic equation.

The Least Squares Approach

An approximate solution for the perturbed velocity potential can be assumed in the form

$$\hat{\phi} = N_i M_k \phi_i^k \tag{35}$$

in which N_i = shape functions in space, M_k = shape functions in time, and ϕ_i^k = unknown parameter corresponding to node i and time level k. Shape functions in space generally depend on the particular element being used as discussed in Section 2. The shape functions in time presently used are the quadratic approximating functions shown in Fig. 9.

Upon substituting Eq. (35) into Eq. (33), the residual R can be expressed in terms of the unknown parameters directly. That is,

$$R = \left[M_k \left(\alpha N_{j,xx} + N_{j,yy} \right) - M_\infty^2 \left(2 M_{k,t} N_{j,x} + M_{k,tt} N_j \right) \right] \phi_j^k \qquad (36)$$

where α is approximated by

$$\alpha = a + b M_\ell N_{p,x} \phi_p^\ell$$

The residual can be rewritten as

$$R = \left(A_j^k + B_j^k \right) \phi_j^k \qquad (37)$$

where

$$A_j^k = M_k \left(\alpha N_{j,xx} + N_{j,yy} \right)$$

$$B_j^k = - M_\infty^2 \left(2 M_{k,t} N_{j,x} + M_{k,tt} N_j \right)$$

The integral expression of

$$\iiint R^2 \, dx \, dy \, dt$$

is minimized with respect to the unknown parameters at time level k = 3, with integration being taken over the physical space and to the time level k = 3.

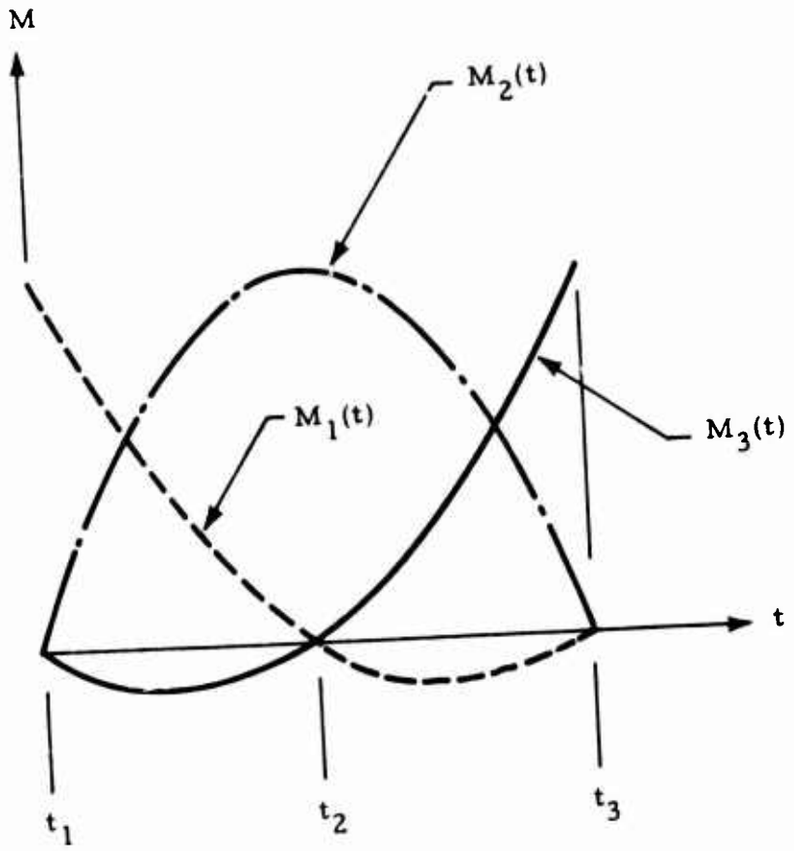

Figure 9 - Shape Functions in Time

That is

$$\frac{\partial}{\partial \phi_j^3} \iiint R^2 \, dx \, dy \, dt = 0$$

or

$$\iiint \frac{\partial R}{\partial \phi_j^3} R \, dx \, dy \, dt = 0 \tag{38}$$

Letting

$$W_i = \frac{\partial R}{\partial \phi_i^3} = A_i^3 + B_i^3 + (M_k N_{j,xx} \phi_j^k) \, bM_3 N_{i,x} \tag{39}$$

the resulting system of algebraic equations becomes

$$\iiint W_i \left[M_k (\alpha N_{j,xx} + N_{j,yy}) - M_k^2 (2 M_{k,t} N_{j,x} + M_{k,tt} N_j) \right]$$

$$\phi_j^k \, dx \, dy \, dt = 0 \tag{40}$$

Equation (40) provides us with a recurrence relation to solve for ϕ_j^3 in terms of ϕ_j^1 and ϕ_j^2.

A program based on Eq. (40) was developed and used to check out first the steady state solutions. Through these numerical experimentations, it was found that, in order to stabilize the time marching scheme, emphasis must be placed on the last time step for terms involving space derivatives only, i.e.,

$$R' = (\alpha' N_{j,xx} + N_{j,yy}) \phi_j^3 - M_\infty^2 (2 M_{k,t} N_{j,x} + M_{k,tt} N_j) \phi_j^k \tag{41}$$

with

$$\alpha' = a + b N_{p,x} \phi_p^3 \tag{42}$$

instead of Eqs. (36) and (37). Such modifications are motivated by observing the implicit finite difference scheme for the wave equation,

$$\phi_{tt} - \lambda^2 \phi_{xx} = 0 \tag{43}$$

Take a pivoting point (i, j), (i denotes x and j denotes t), assume mesh size in x is k and in t is h, then the difference equation is

$$\frac{\phi_{i,j} - 2\phi_{i,j-1} + \phi_{i,j-2}}{h^2} - \lambda^2 \frac{\phi_{i+1} - 2\phi_{i,j} + \phi_{i-1,j}}{k^2} = 0 \qquad (44)$$

Through Von Newmann's stability analysis by Fourier series (Ref. 15), this equation can be shown to be unconditionally stable for all λ, h and k. An immediate observation is that ϕ_{xx} is differenced in the x direction at the last time step. Since the left-hand side of the finite difference equation (44) is in fact the residual at a discrete node, the analogous residual for the present transonic equation via finite element approach therefore is Eq. (41). Note that $M_k \phi_j^k$ in Eq. (36) is replaced by $(M_1 + M_2 + M_3)\phi_j^3$ in Eq. (41), which reduces to ϕ_j^3, since $M_1 + M_2 + M_3 = 1$.

With the residual established, the corresponding weighting functions can be readily determined, thus leading to the required system of algebraic equations.

It remains to argue that

$$\Delta R = R - R' = \left[M_2 (\phi_j^3 - \phi_j^2) + M_1 (\phi_j^3 - \phi_j^1)\right] N_{j,yy}$$

$$+ \left[M_1 (\alpha\phi_j^1 - \alpha'\phi_j^3) + M_2 (\alpha\phi_j^2 - \alpha'\phi_j^3)\right. \qquad (45)$$

$$\left. + M_3 (\alpha - \alpha')\phi_j^3\right] N_{j,xx}$$

If steady flow is approached,

$$\phi_3 = \phi_2 = \phi_1, \ \alpha = \alpha' \Longrightarrow \Delta R = 0 \qquad (46)$$

Therefore this approach is appropriate for computing steady flow. In this case, the role of ΔR seems to be the same as the numerical viscosity term introduced in the implicit finite difference scheme through truncation.

Other aspects of the numerical approach are similar to what was described in Section 2.2 for steady flow, except that the boundary conditions imposed along the branch cut are noticeably different. Also, a process of marching in time is taken, instead of successive iterations used on the steady counterpart.

Along the branch cut (vortex sheet in unsteady flow), Eqs. (26) and (27) must be imposed to ensure the continuity of pressure and downwash. To impose the first condition, Eq. (26), for a pair of nodes along the branch cut, the two finite element equations generated originally for $\phi^+_{,x}$ and $\phi^-_{,x}$ are properly combined to yield one equation, while the equation for $\phi^+_{,x}$ is replaced by the following equation, evaluated at time level $t = t_3$:

$$\phi^{+(3)}_{,x} - \phi^{-(3)}_{,x} + M_{3,t}\,(\phi^{+(3)} - \phi^{-(3)}) = M_{2,t}\,(\phi^{-(2)} - \phi^{+(2)}) + M_{1,t}\,(\phi^{-(1)} - \phi^{+(1)}) \qquad (47)$$

Where M is the shape function in time and the superscripts denote the time steps, while solutions for the first and the second time steps are known.

Equation (27) can be imposed in a similar fashion. This condition, within the limit of small perturbation assumption, will ensure flow just above and below the branch cut behaves as an unsteady vortex sheet, and in the steady case this vortex sheet will vanish eventually.

3. NUMERICAL RESULTS

As mentioned earlier, the Galerkin approach was found to be invalid for computing critical transonic flows and hence abandoned. As an alternative, the least squares approach was pursued and applied to compute both steady and unsteady transonic flows. Results obtained thus far indicate that the least squares approach is generally very satisfactory. Computations

performed using the unsteady code are presented and discussed in the following.

Steady Transonic Flow over a 6% Thick Circular Arc

In order to debug the unsteady code and study the feasibility of the present approach, steady state solutions for flow over a 6% thick circular arc airfoil were first computed and compared to those obtained previously by solving the steady transonic equation. The mesh used in the computations is shown in Fig. 10, where the typical time step used is $\Delta t = 1$.

The case of $M_\infty = 0.861$ (barely critical) was computed first. Convergent solutions was obtainable whether or not an improper downwind influence on the solution at an upwind station in the supersonic pocket is discarded or not. The two solutions are unnoticeably different. This is obviously because, for $M_\infty = 0.861$, the local supersonic region is very small and therefore the effect of the improper upwind influence is insignificant. Shown in Fig. 11 are results eliminating the downwind influence and compared with experimental results (Ref. 13).

For cases with higher freestream Mach number, however, numerical solutions corresponding to with and without downwind influence in the spatial direction are definitely different. Solution with improper downwind influence removed produces a shock wave, although somewhat smeared; while the other case yields a shockless solution with flow expanded and recompressed smoothly throughout the supersonic pocket. The latter results had also been observed in the steady equation formulation, when downwind influence was retained and Newton-Raphson's method was used to solve the nonlinear algebraic equations. Nevertheless, solution of the latter type (shockless flow) is considered to be hydrodynamically incorrect due to considerations of entropy production through shocks. For this reason, the scheme with improper downwind influence removed in the supersonic region is adapted. Results for the cases of $M_\infty = 0.909$ and $M_\infty = 0.966$ are also shown in Fig. 11 and compared with experimental data due to Knechtel (Ref. 13). It is seen that the shock position for the two cases is

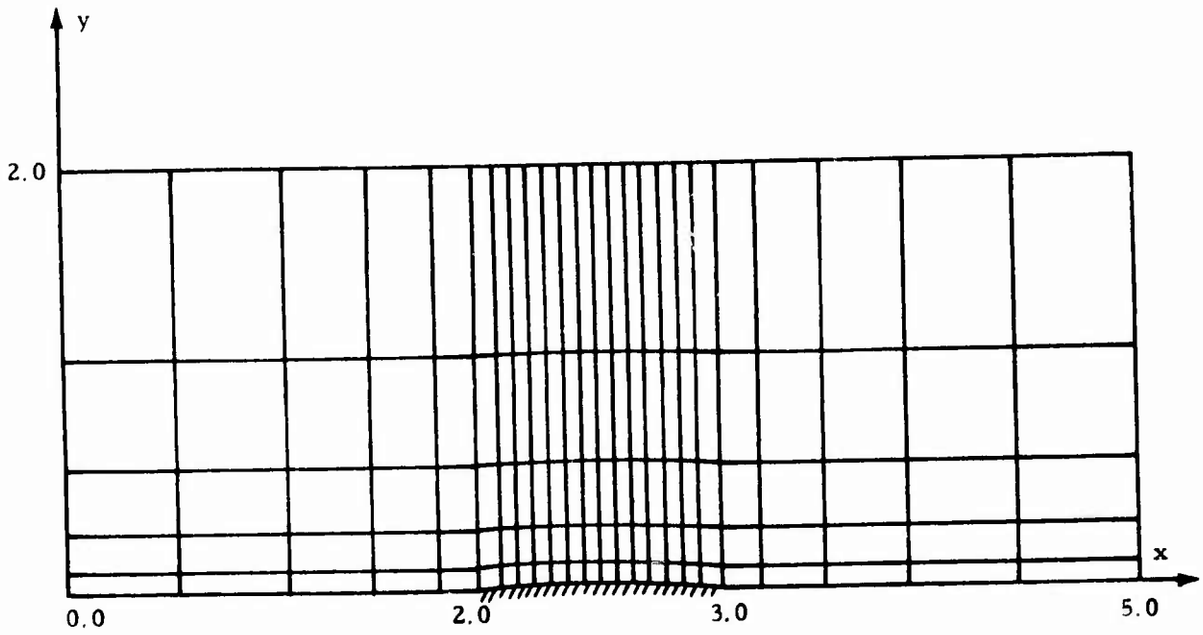

Figure 10 - Finite Element Representation for Flow past a Thin Airfoil in a Wind Tunnel (120 Elements, 150 Nodes)

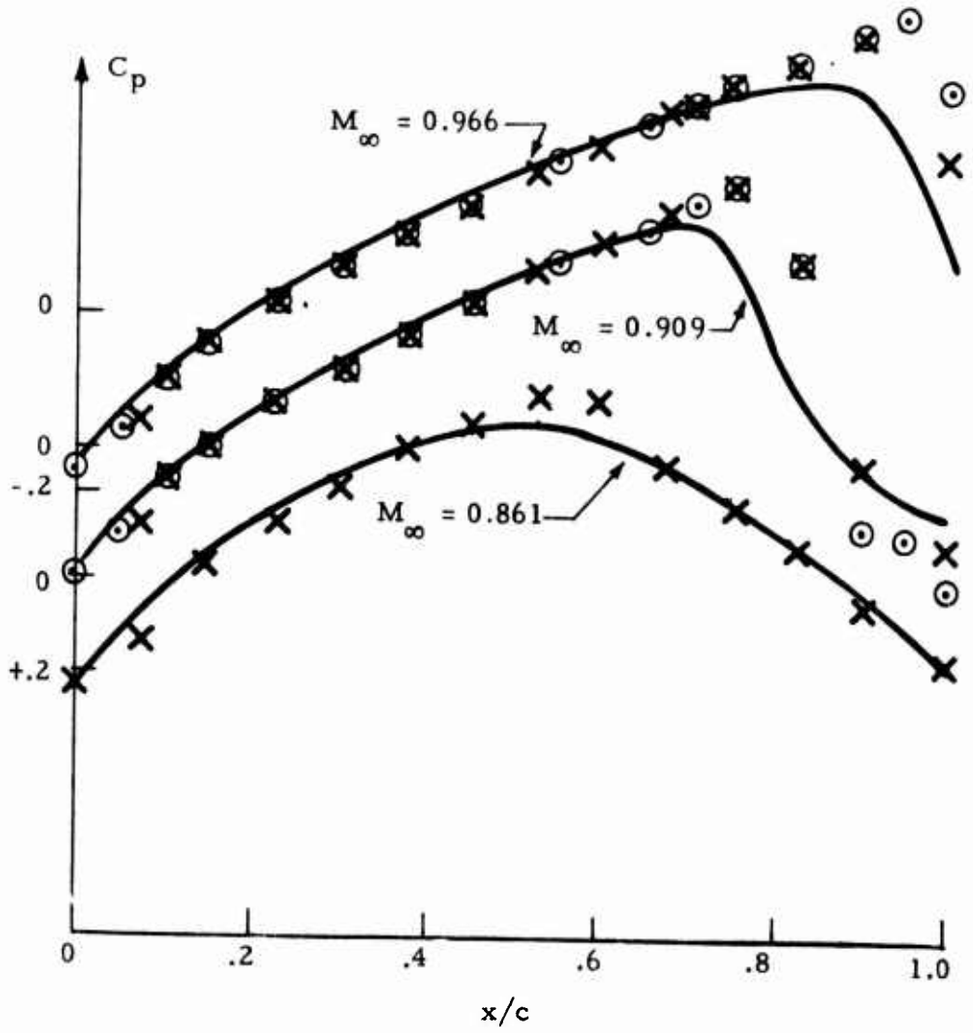

Figure 11 - Comparison of Chordwise Pressure Distribution for a 6% Thick Circular-Arc Airfoil (α = 0 deg)

somewhat behind that found in experiment, a fact also observed in finite difference calculations. In our numerical scheme, shock continuity has not been treated as such, and the shock was smeared at least within the width of the element where the shock is supposed to be located. A simple way to obtain a better resolution is to refine the mesh in the recompression region.

On attempting to refine the solutions for $M_\infty = 0.909$ and 0.966, a mesh layout depicted in Fig. 12 was used. The results for the case of $M_\infty = 0.909$ agree very well with those obtained from using the coarser mesh, except for flow after the shock, where recompression is stronger for the finer mesh. This is expected, when the mesh is refined the (smeared) shock is confined within a smaller region, and better resolution should result. For the case of $M_\infty = 0.966$, the shock was also found to be closer to the trailing edge, compared with the solution obtained using the coarser mesh. The present results appear to agree with Murman's recent finding (Ref. 14) about embedded shock over airfoil. He observed that when FCR (fully conservative relaxation) is used, the solution gives stronger shocks that are farther aft on the airfoil compared with that using the NCR (not fully conservative relaxation). For reference, his discussion on why NCR agrees better with experimental results than FCR may be consulted.

Unsteady Transonic Flow over a NACA 64 A006 Airfoil

To demonstrate the applicability of the present approach, several cases of unsteady transonic flow over a NACA 64 A006 airfoil were studied. The airfoil is assumed at zero incidence but with a quarter chord flap executing harmonic motion. The cases studied include

$$M_\infty = 0.794, \quad k = 0.064$$
$$M_\infty = 0.804, \quad k = 0.253$$
$$M_\infty = 0.901, \quad k = 0.057$$
$$M_\infty = 0.903, \quad k = 0.228$$

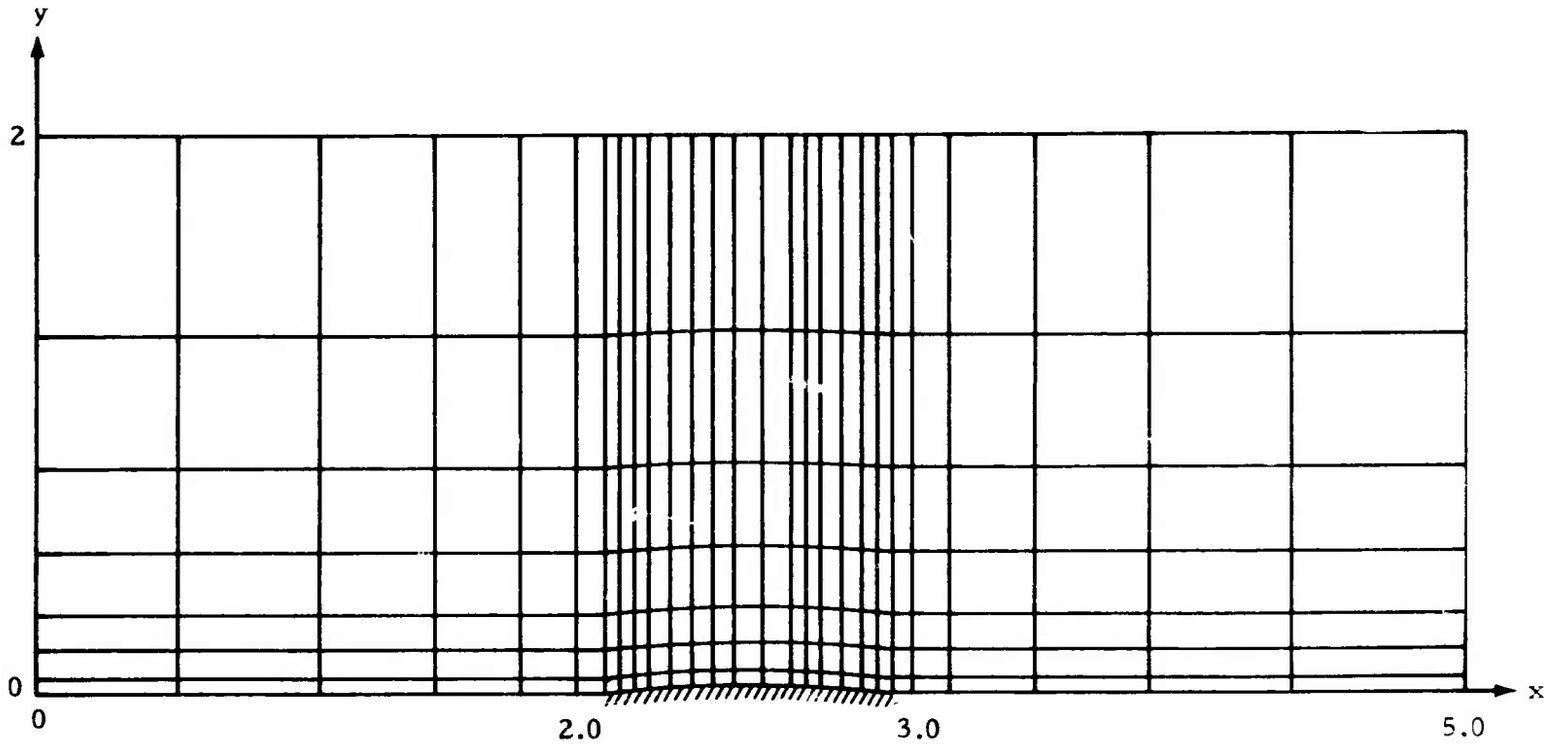

Figure 12 - Finite Element Representation for Flow Past a Thin Airfoil in a Wind Tunnel (189 Elements, 224 Nodes)

The element mesh used is shown in Fig. 13, consisting of 165 elements with 198 nodes. For each cycle of oscillation, 16 time steps were used in the computations. For the two supercritical cases, M_∞ = 0.901 and 0.903, unlike their steady counterparts, the special "one-sided assembly" scheme was not necessary in the computations, and harmonic solutions are apparently obtained in two cycles of computations.

Numerical results including the unsteady pressure jump at typical stations (x/c = 0.725 and 0.775) and the amplitude of the unsteady pressure difference over the airfoil are depicted and compared in Figs. 14 through 25. In these figures, the pressure is normalized with respect to the angle θ, the amplitude of flap oscillation. The experimental data are reported by Tijdeman and Schippers (Ref. 16). In general the agreement for predicted results and experimental data is very good. In particular, results for the typical stations (x/c = 0.725 and 0.775) near the hinge point show excellent agreement in both magnitude and phase angle. The amplitude of the unsteady pressure difference over the airfoil is also depicted with the comparisons made. Again, the experimental data have been converted to yield the value of amplitude. The dashed line in the figure corresponds to results obtained earlier by an approach developed for NASA-Langley (Ref. 6), assuming the unsteadiness to be a small perturbation to the mean steady flow. Note that the results obtained by the two theoretical approaches agree very well over most parts of the airfoil; and agreement between present results and experimental data is very good for the aft half of the airfoil. Close to the leading edge, both finite element solutions appear to under-predict the amplitude of unsteady pressure jump. Many factors could attribute to this fact. The small perturbation assumption currently used requires that flow be only slightly perturbed from uniform flow. Consequently, the flow behavior in the vicinity of a leading edge stagnation point cannot be correctly represented with such an assumption. The coarseness of the present mesh may also cause inaccuracy, especially near the leading edge. Furthermore, the assumption of no disturbance along the outer boundary of the mesh as used in the present computations is considered to have a tendency to suppress the development of a pressure jump, especially for the leading edge region, where no oscillation is taking place.

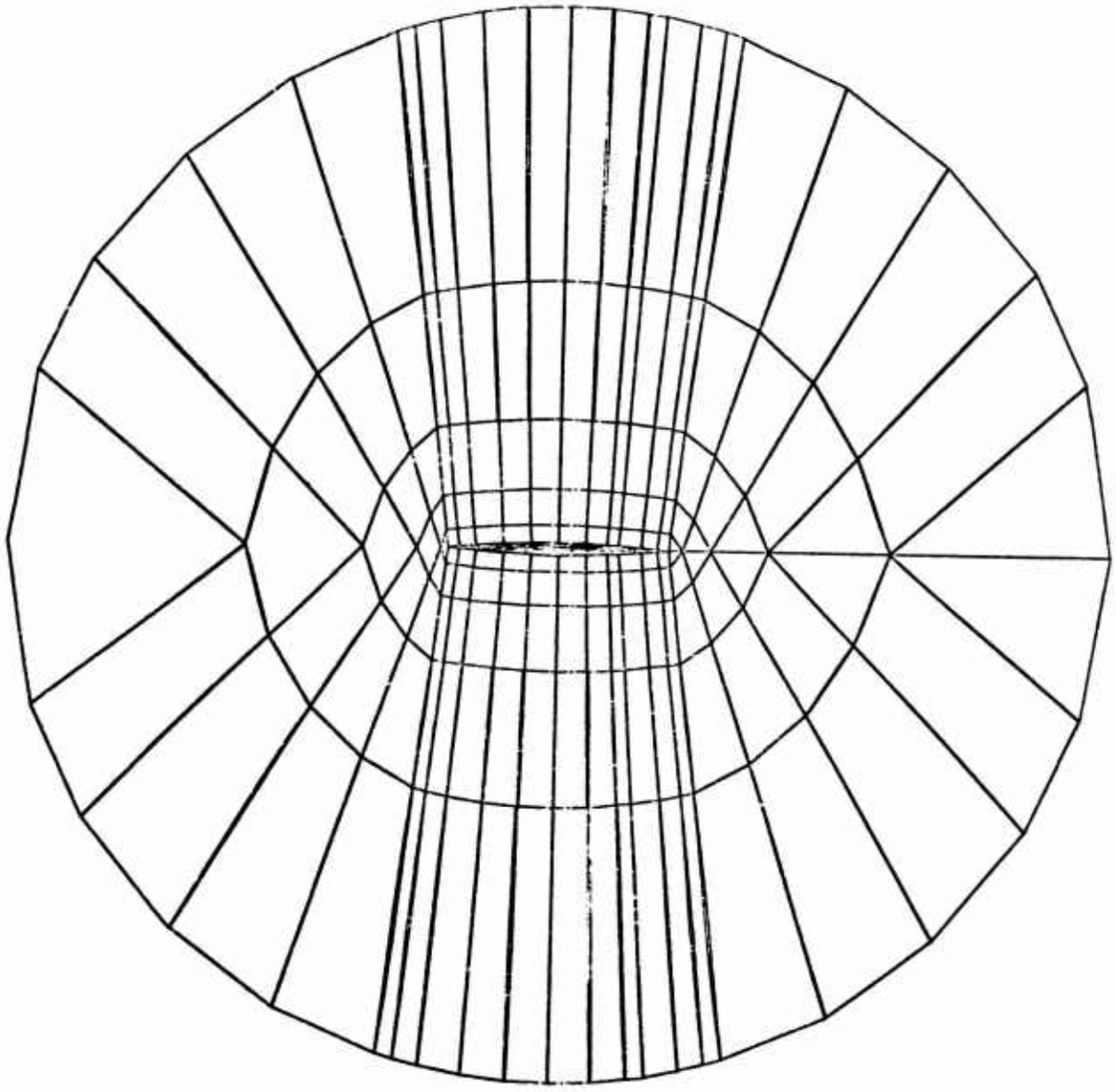

Fig. 13 - Finite Element Mesh (165 Elements, 198 Nodes)

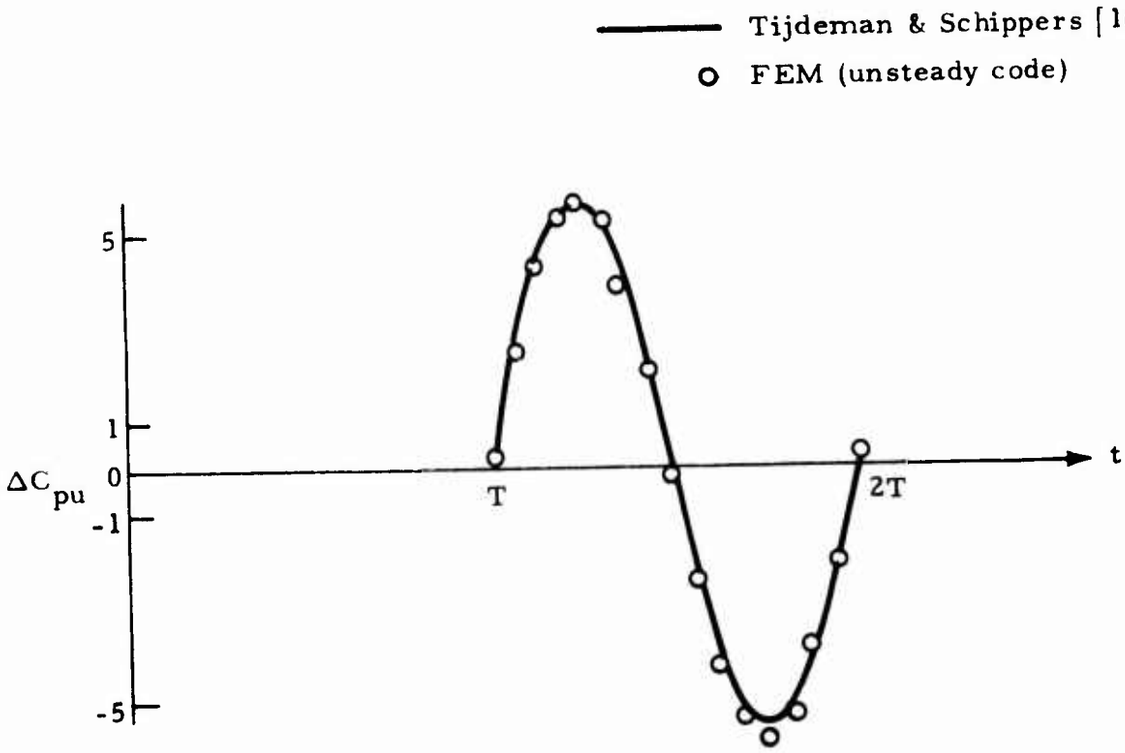

Figure 14 - Time History of Unsteady Pressure at x/c = 0.725
(M_∞ = 0.794, k = 0.064)

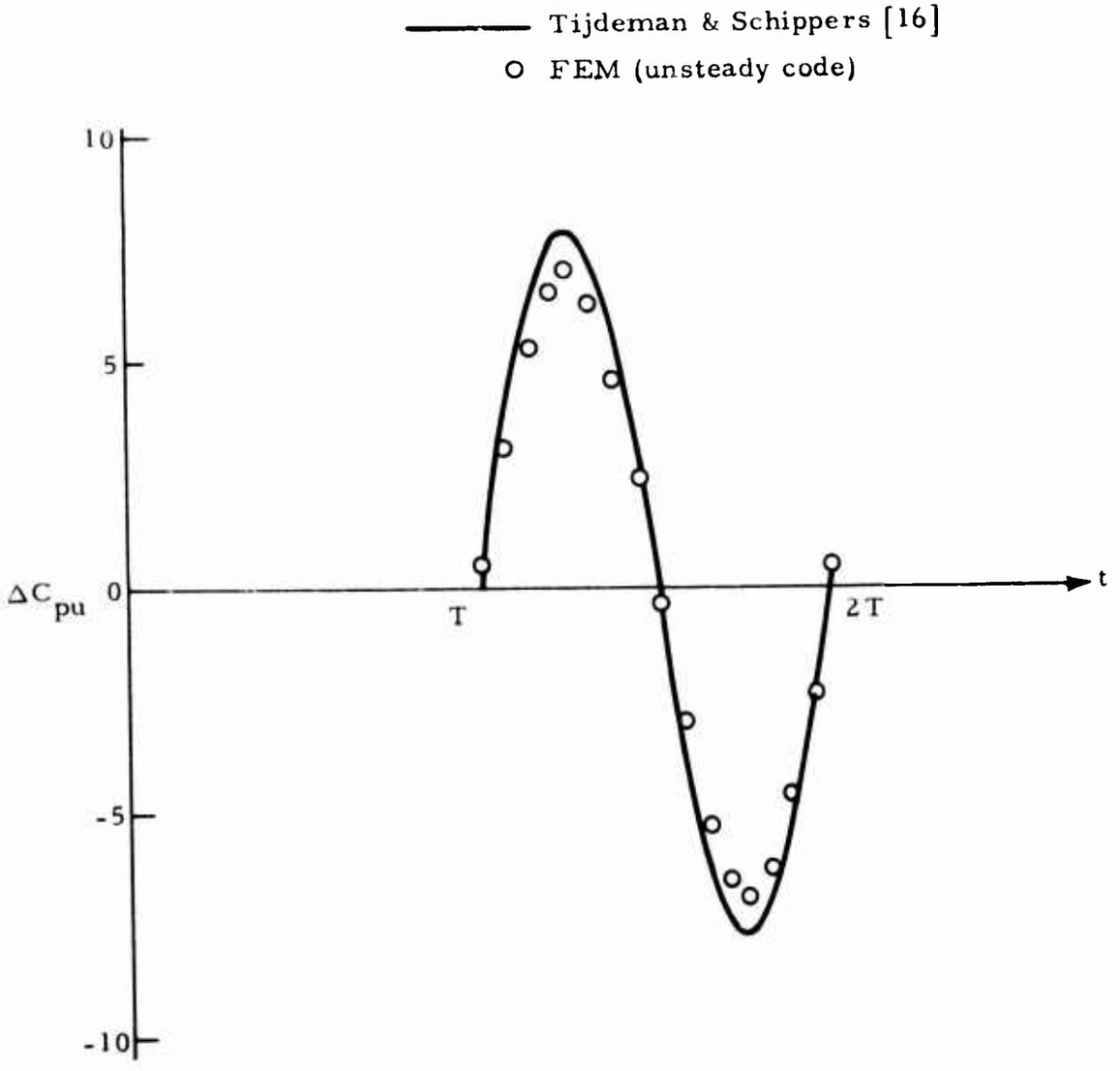

Figure 15 - Time History of Unsteady Pressure at x/c = 0.775
(M_∞ = 0.794, k = 0.064)

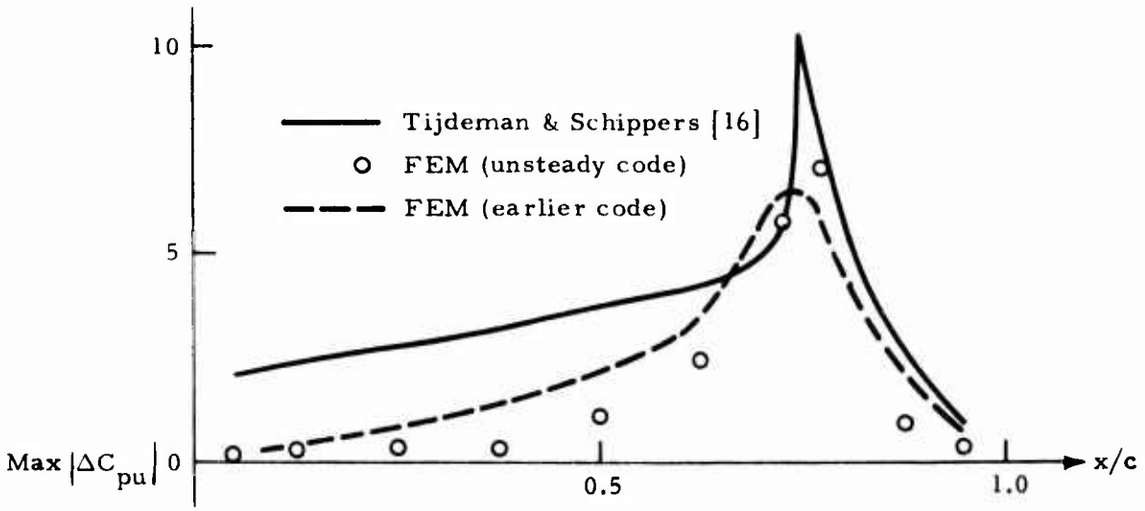

Figure 16 - Amplitude of Unsteady Pressure on Airfoil
(M_∞ = 0.794, k = 0.064)

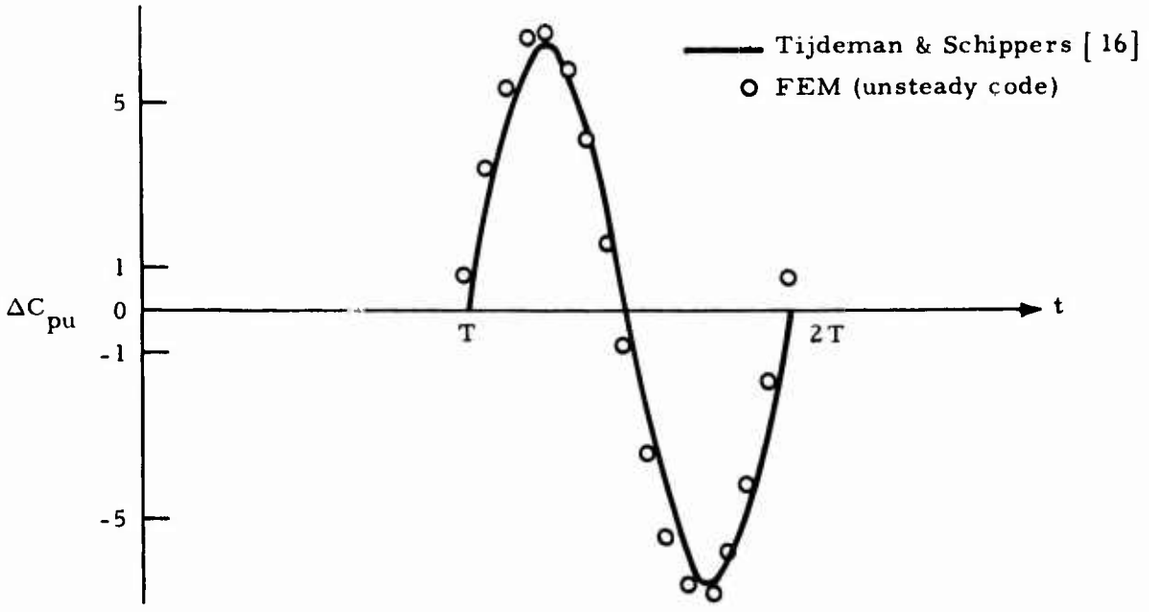

Figure 17 - Time History of Unsteady Pressure at x/c = 0.725
(M_∞ = 0.804, k = 0.253)

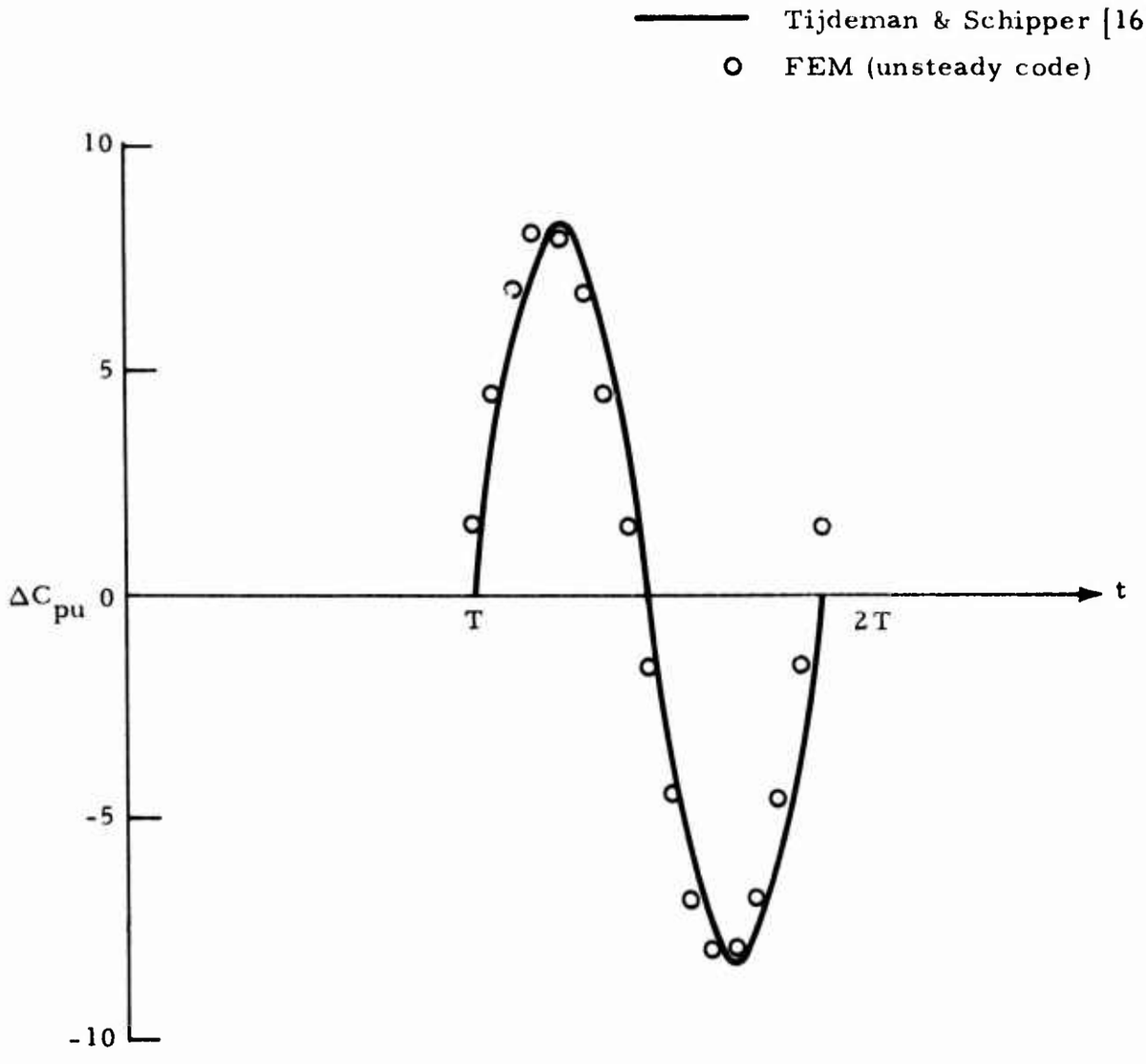

Figure 18 - Time History of Unsteady Pressure at x/c = 0.775
(M_∞ = 0.804, k = 0.253)

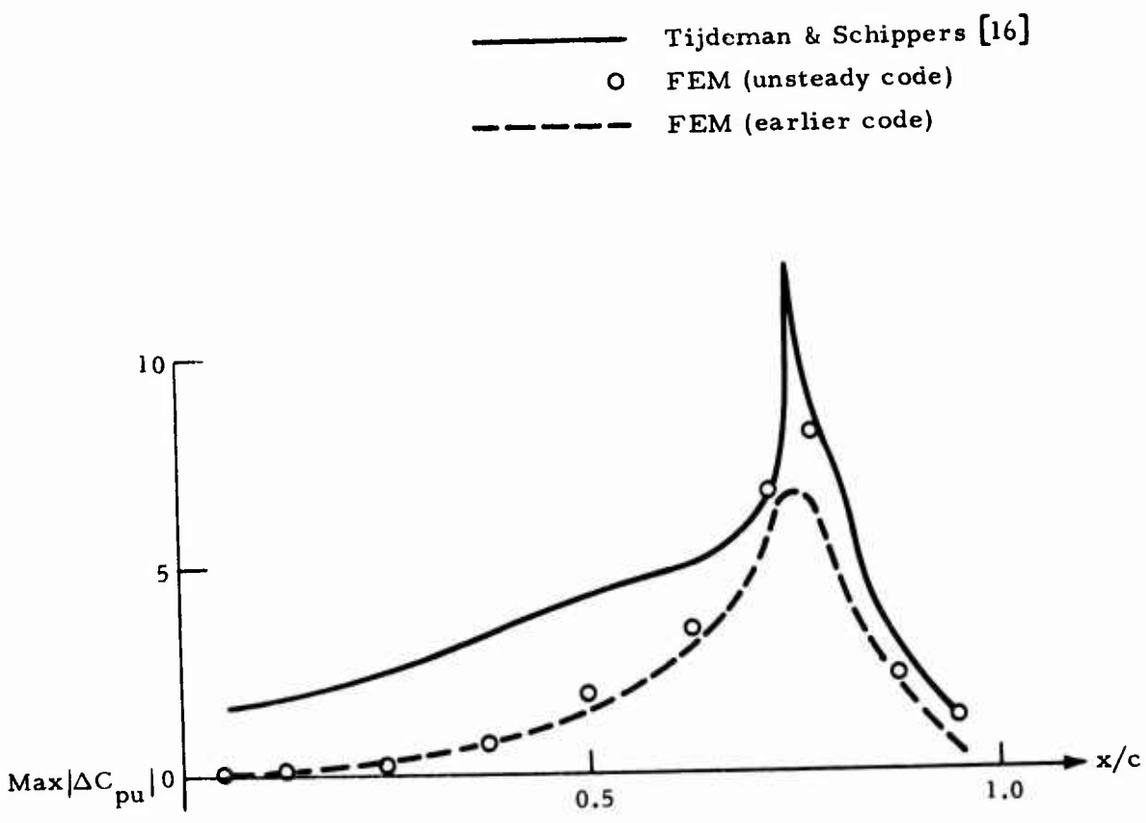

Figure 19 - Amplitude of Unsteady Pressure on Airfoil
(M_∞ = 0.804, k = 0.253)

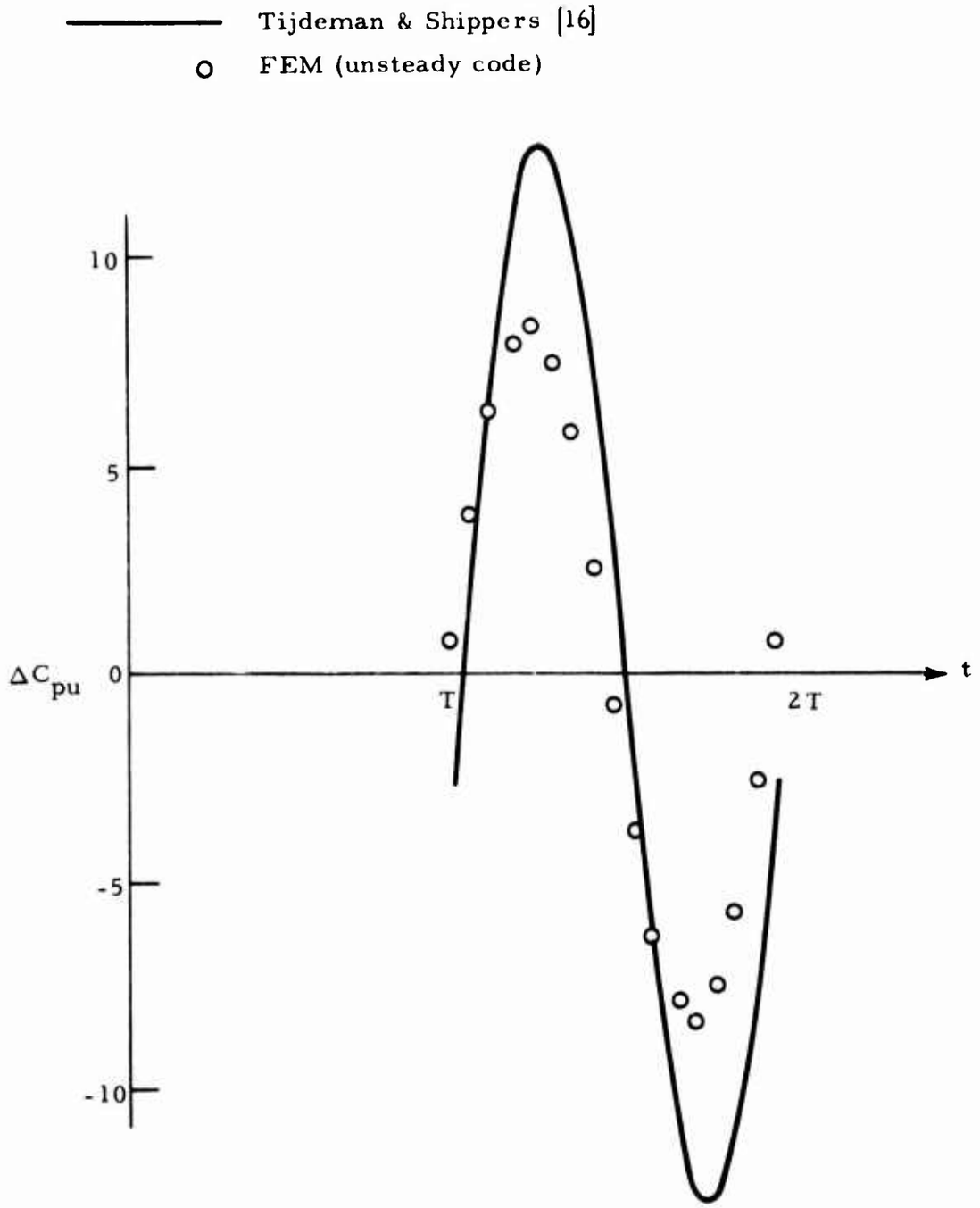

Figure 20 - Time History of Unsteady Pressure at x/c = 0.725
(M_∞ = 0.901, k = 0.057)

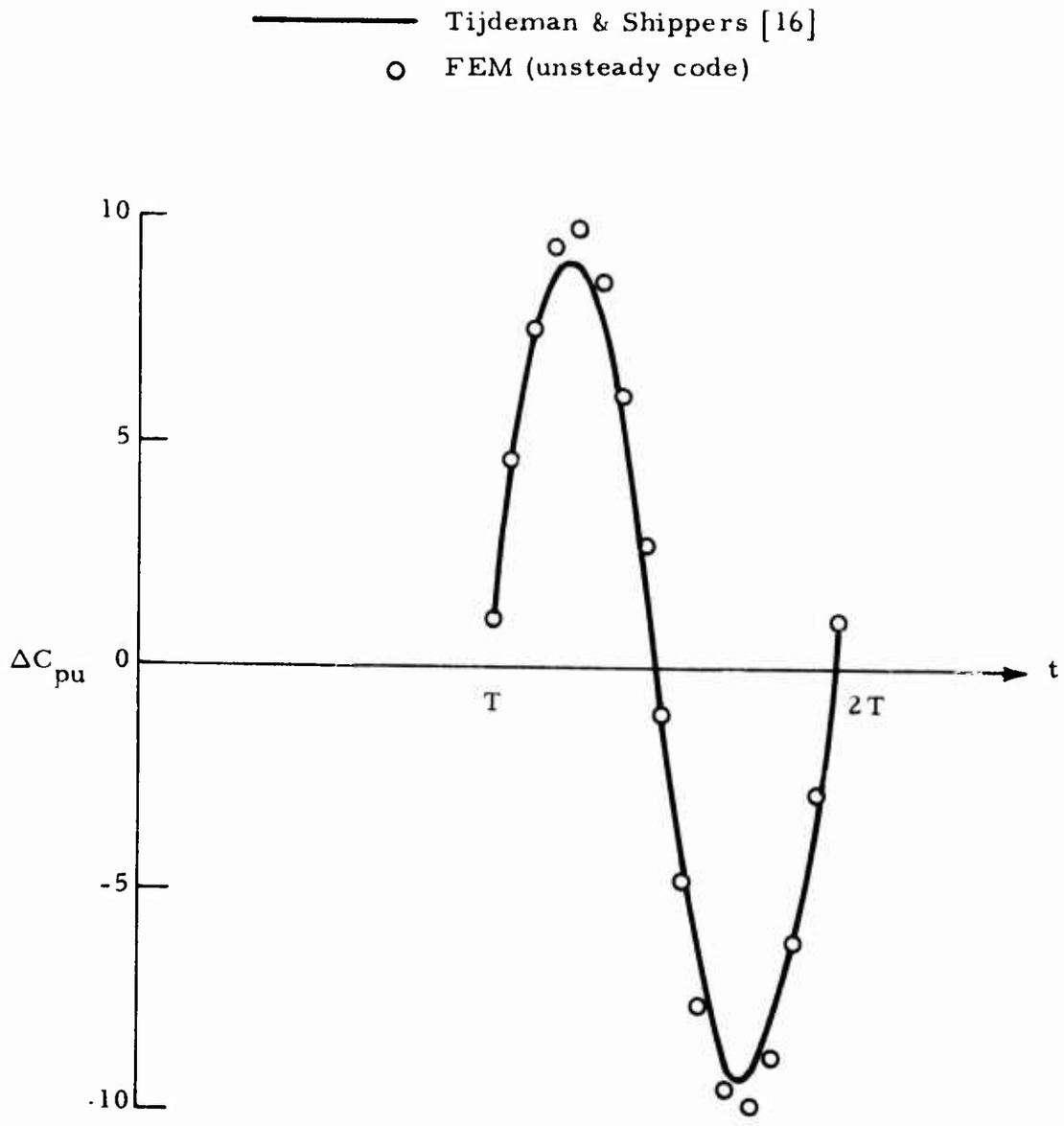

Figure 21 - Time History for Unsteady Pressure at x/c = 0.775 (M_∞ = 0.901, k = 0.057)

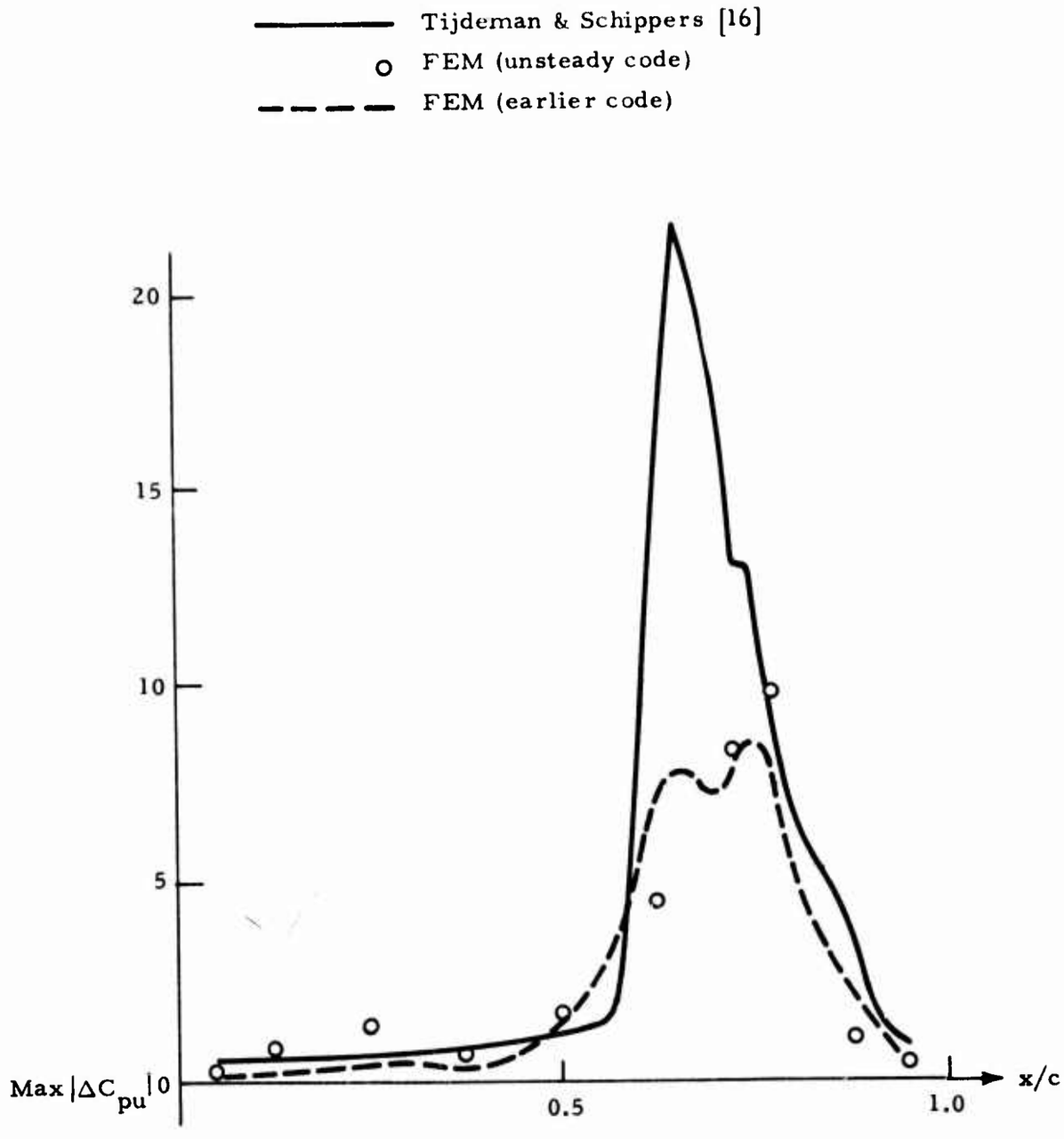

Figure 22 - Amplitude of Unsteady Pressure on Airfoil
(M_∞ = 0.901, k = 0.057)

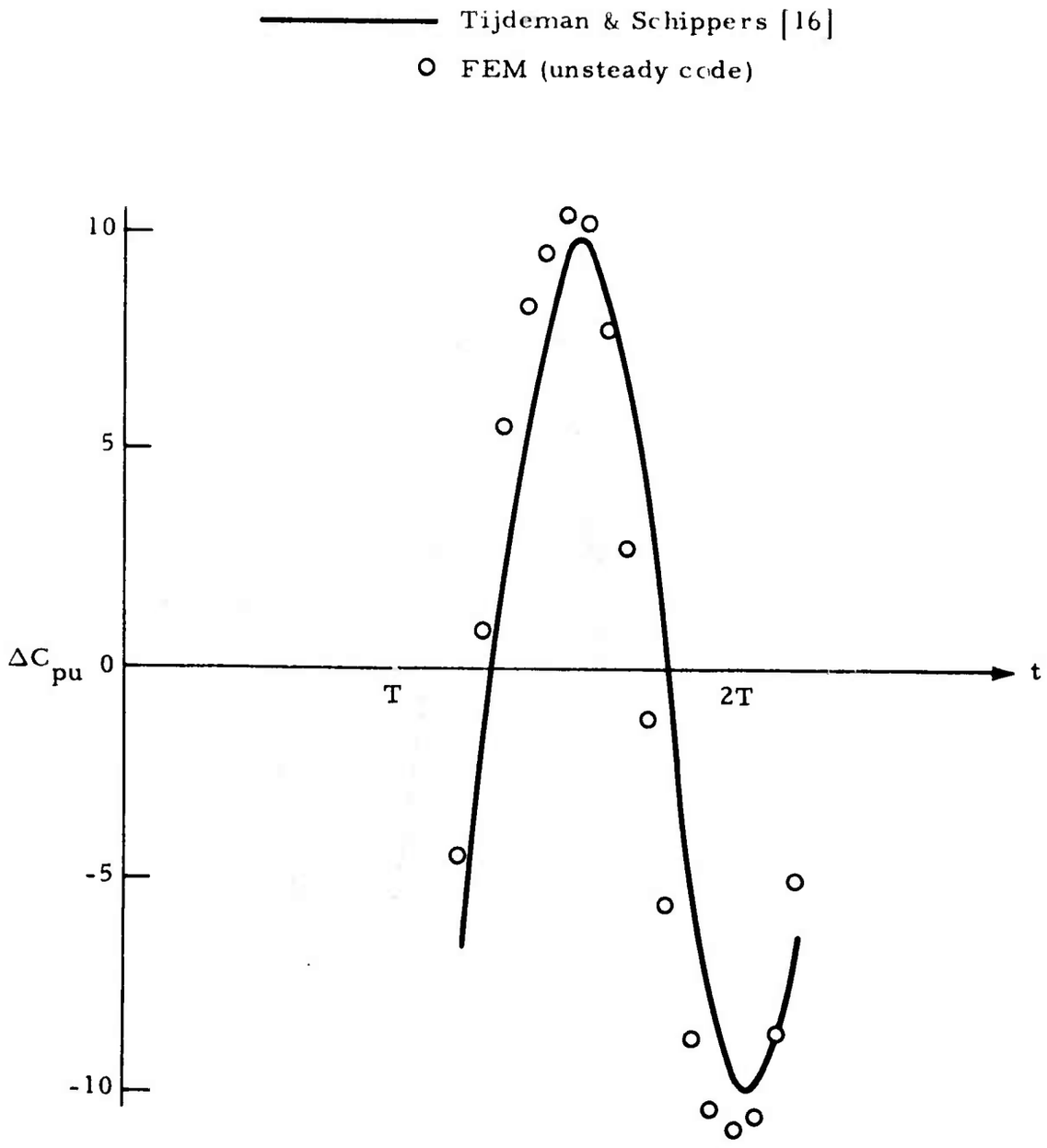

Figure 23 - Time History of Unsteady Pressure at x/c = 0.725 (M_∞ = 0.903, k = 0.228)

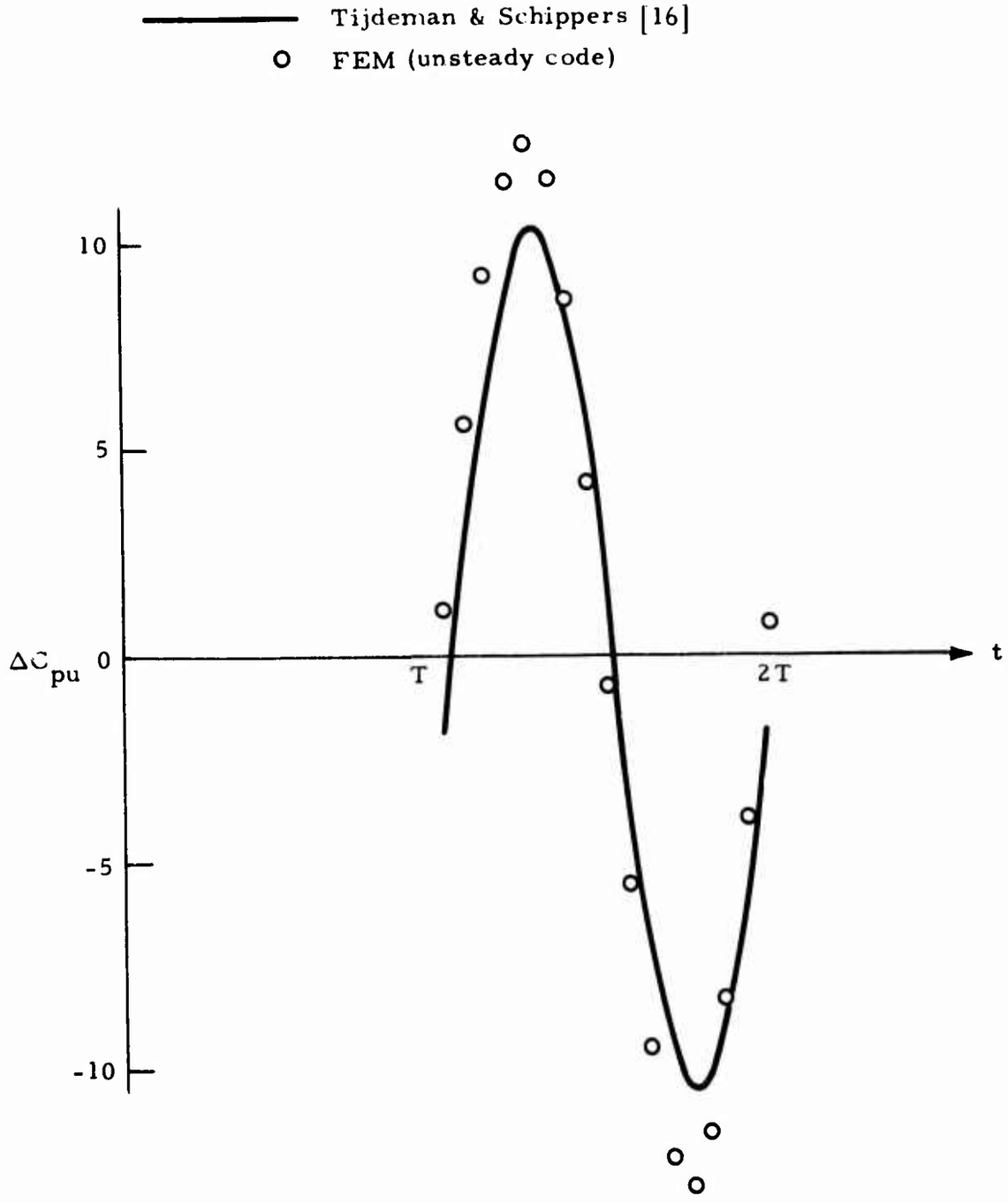

Figure 24 - Time History of Unsteady Pressure at x/c = 0.775
(M_∞ = 0.903, k = 0.228)

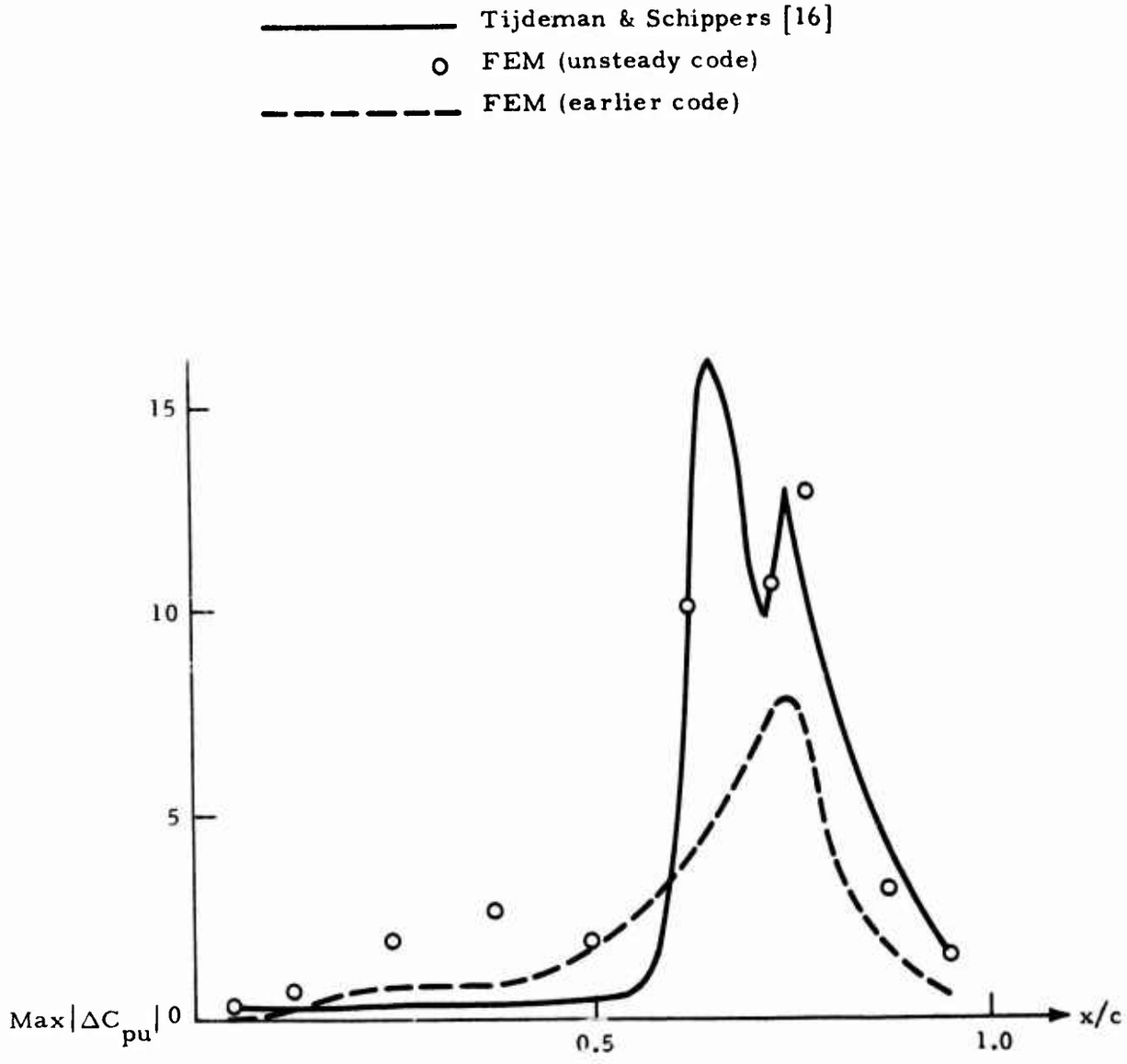

Figure 25 - Amplitude of Unsteady Pressure on Airfoil
(M_∞ = 0.903, k = 0.228)

It is seen from the predicted results that the present approach is suited for computing unsteady transonic flows and steady flow as well. For an airfoil undergoing harmonic motion, oscillatory solution is obtainable in two to three cycles, and requires only moderate computation time. For the mesh presently used, marching in time one step forward requires approximately 40 seconds CPU time on a Univac 1108 computer, and each case requires about 10.5 minutes for completing computations for one cycle, with 16 time steps. As the present computer program has not been optimized yet, some reduction in computation time is still possible.

SECTION IV
CONCLUSIONS AND RECOMMENDATIONS

The work presented in this report represents an initial attempt toward developing a general numerical method for computing steady and unsteady transonic flows over thin airfoils based on small disturbance theory. Unlike other existing approaches for calculating unsteady transonic flows, the present numerical algorithm solves directly the unsteady transonic equation with both time derivative terms retained in the computations. Thus the present algorithm can be applied to compute a much wider class of transonic flow problems, including steady, oscillatory or transient solutions, either with or without angle of attack. For oscillatory flow, no assumption is made regarding the oscillating frequencies, nor is the unsteady perturbation necessarily to be small compared to the mean steady solution.

The present numerical algorithm is developed using the finite element concept in conjunction with the least squares method of weighted residuals applied to both space and time. Also, schemes for handling mixed flows and problems involving an infinite domain have been developed and implemented in the present numerical method. These newly developed schemes, together with the advantages offered by the finite element technique which includes great flexibility in mesh arrangement, ease with implementing higher order approximations, and its effectiveness in treating complex geometry and boundary conditions, etc., make the present approach feasible and should prove to be definite assets in computing more complicated transonic flow problems.

The developed procedures have been applied to solve several problems of steady and unsteady transonic flows over thin airfoils, and results obtained compare generally very well with experimental data and those obtained by other numerical techniques. Regarding computational efficiency, only moderate

computation time is needed, even the most time consuming case requires only about ten minutes CPU time on a CDC 6600 computer. These exploratory studies well indicate the feasibility and applicability of the finite element approach for computing steady and unsteady transonic flows. However, as the effort to date has concentrated on investigating the best suited finite element approach, little consideration has been given to optimize the computational efficiency and to certain details, such as more accurate treatment of the leading edge singularity and unsteady effects along the outer boundary. These refinements are apparently desirable and certainly could be accomplished. In addition to these improvements, it is recommended that further study be pursued in the following areas:

a. Some studies need to be done on the effects of "non-conforming" versus "conforming" elements. As is known, the elements presently used are C^1 continuous only at nodal points, but not across element boundaries, which apparently violates C^1 continuity between elements as normally required. Although our experiences and numerical results indicate that the use of "non-conforming" elements do not cause problems with convergence, as concluded in plate bending analysis, some studies on the effects of "non-conforming" versus "conforming" elements are apparently highly desirable and useful, considering the fact that the present problem is nonlinear and involves equations of the mixed elliptic-hyperbolic type. "Conforming" elements do exist and could be readily implemented. This study could be conducted concurrently with the development of a more sophisticated scheme for handling shock waves, such as shock-fitting.

b. The procedures developed in this study could be extended without too much effort to treat problems involving multi-element airfoils and the cascade problem. As techniques for handling shock waves (by smearing) and Kutta conditions in the wake have already been developed and appear to work well for a single airfoil, the anticipated major effort in solving the problem of multi-element airfoils and cascades would be to develop or implement some efficient scheme for solving a large system of algebraic equations, such as an out-of-core equation solver. Alternatively, a scheme based on the concept of line relaxation, as extensively used in finite difference techniques, could be developed to cope with the problem.

c. It is desirable and apparently feasible to develop a finite element algorithm to solve the nonlinear full potential equation, as the versatility of the method can be more effectively utilized for such a problem. Another possibility is to solve the two-dimensional unsteady Euler equations directly and at the end include also the viscous effects.

Finite difference relaxation techniques for solving these equations have already been developed; however, tremendous computation time is usually required even for solving a two-dimensional problem. In the light of fully utilizing the advantages offered by the finite element method, such as great flexibility in mesh arrangement, ease with implementing higher order approximations, and its effectiveness in treating complex geometry and boundary conditions, the method could lead to higher computational efficiency than other existing numerical techniques. Through these studies, the feasibility of using finite element methods to solve the three-dimensional and more difficult transonic flow problems can also be assessed.

REFERENCES

1. Bland, S.R., "Recent Advances and Concepts in Unsteady Aerodynamic Theory," Aerodynamic Analyses Requiring Advanced Computers, Part II, NASA SP-347, Langley Research Center, Hampton, Va., 1975, pp. 1305-1326.

2. Chan, S.T.K., M.R. Brashears and V.Y.C. Young, "Finite Element Analysis of Transonic Flow by the Method of Weighted Residuals," Paper 75-79, AIAA 13th Aerospace Sciences Meeting, Pasadena, Calif., January 1975.

3. Traci, R.M., E.D. Albano et al., "Small Disturbance Transonic Flows About Oscillating Airfoils," AFFDL-TR-74-37, Wright-Patterson AFB, Ohio, June 1974.

4. Ehlers, F.E., "A Finite Difference Method for the Solution of the Transonic Flow Around Harmonically Oscillating Wings," NASA CR-2257, January 1974.

5. Ballhaus, W.F., R. Magnus and H. Yoshihara, "Some Examples of Unsteady Transonic Flows over Airfoils," Proceedings of the Symposium on Unsteady Aerodynamics, Vol.II, University of Arizona, 18-20 March 1975, pp. 769-791.

6. Chan, S.T.K., and M.R. Brashears, "Analysis of Steady and Unsteady Transonic Flows by Finite Element Method," NASA CR-144930, February 1976.

7. Chan, S.T.K., and M.R. Brashears, "Computer Program for Steady Transonic Flow over Thin Airfoils by Finite Elements," AFFDL-TR-75-126, October 1975.

8. Bazeley, G.P., Y.K. Cheung, B.M. Irons and O.C. Zienkiewicz, "Triangular Elements in Plate Bending — Conforming and Non-Conforming Solutions," Proc. of First Conf. on Matrix Methods in Struc.Mech., Wright-Patterson AFB, Ohio, 1965, pp. 547-576.

9. Sells, C.C.L., "Plane Subcritical Flow past a Lifting Airfoil," Proc.Roy. Soc. (London), Series A, Vol 308, No. 1494, 1968, pp. 377-401.

10. Murman, E.M., and J.D. Cole, "Calculation of Plane Steady Transonic Flows," AIAA J., Vol. 9, No. 1, January 1971, pp. 114-121.

11. Krupp, J.A., "The Numerical Calculation of Plane Steady Transonic Flows past Thin Lifting Airfoils," D180-12958-1, The Boeing Company, June 1971.

12. Klunker, E.B., "Contribution to Methods for Calculating the Flow About Thin Lifting Wings at Transonic Speeds — Analytic Expression for the Far Field," NASA TN-D-6530, November 1971.

13. Knechtel, E.D., "Experimental Investigation at Transonic Speeds of Pressure Distributions over Wedge and Circular-Arc Airfoil Sections and Evaluation of Perforated-Wall Interference," NASA TN D-15, August 1959.

14. Murman, E.M., "Analysis of Embedded Shock Waves Calculated by Relaxation Methods," AIAA J., Vol. 12, No. 5, May 1974, pp. 626-633.

15. O'Brien, G.G., M.A. Hyman and S. Kaplan, "A Study of the Numerical Solution of Partial Differential Equations," J. Math. Phys., Vol. 29, 1951, pp. 223 251.

16. Tijdeman, H., and P. Schippers, "Results of Pressure Measurements on an Airfoil with Oscillating Flap in Two-Dimensional High Subsonic and Transonic Flow," NLR-TR 73078, (U) 1973.

☆ U. S. GOVERNMENT PRINTING OFFICE: 1976 — 657-630/855